IMPLEMENTATION OF TURBULENCE MODELS INTO A NAVIER-STOKES
SOLVER

A THESIS SUBMITTED TO
THE GRADUATE SCHOOL OF NATURAL AND APPLIED SCIENCES
OF
MIDDLE EAST TECHNICAL UNIVERSITY

BY

MUSTAFA YILMUŞTA

IN PARTIAL FULFILLMENT OF THE REQUIREMENTS
FOR
THE DEGREE OF MASTER OF SCIENCE
IN
MECHANICAL ENGINEERING

SEPTEMBER 2004

Approval of the Graduate School of Natural and Applied Sciences

———————————————

Prof. Dr. Canan ÖZGEN
Director

I certify that this thesis satisfies all the requirement as a thesis for the degree of Master of Science.

———————————————

Prof. Dr. S. Kemal İDER
Head of Department

This is to certify that we have read this thesis and that in our opinion it is fully adequate, in scope and quality, as a thesis for the degree of Master of Science.

———————————————

Prof. Dr. M. Haluk AKSEL
Supervisor

Examining Committee Members

Prof. Dr. Kahraman ALBAYRAK	(METU, ME)	———————————
Prof. Dr. M. Haluk AKSEL	(METU, ME)	———————————
Asst. Prof. Dr. Tahsin ÇETİNKAYA	(METU, ME)	———————————
Asst. Prof. Dr. Cüneyt SERT	(METU, ME)	———————————
Ruşen ÇETE (M.Sc. in ME)	(TAI)	———————————

I hereby declare that all information in this document has been obtained and presented in accordance with academic rules and ethical conduct. I also declare that, as required by these rules and conduct, I have fully cited and referenced all material and results that are not original to this work.

Mustafa Nail Muşta

ABSTRACT

IMPLEMENTATION OF TURBULENCE MODELS INTO A NAVIER-STOKES
SOLVER

MUŞTA, Mustafa Nail

M.Sc., Department of Mechanical Engineering

Supervisor: Prof. Dr. M. Haluk Aksel

September 2004,91 pages

In order to handle turbulent flow problems, one equation turbulence
models are implemented in to a previously developed explicit, Reynolds averaged
Navier-Stokes solver. Discretization of Navier-Stokes solver is based on cell-
vertex finite volume formulation combined with single step Lax-Wendroff
numerical method which is second order accurate in space. Turbulent viscosity
is calculated by using one equation Spalart-Allmaras and Baldwin-Barth
turbulence transport equations. For the discretization of Spalart-Allmaras and
Baldwin-Barth equations, both finite volume scheme which is used for Navier-
Stokes equation in this work and explicit finite difference discretization method
are used.

In order to increase the convergence rate of the solver, local time
stepping technique is applied. Stabilization of non-physical oscillations

resulting from the numerical scheme is maintained by adding second and fourth order artificial smoothing terms.

Three test cases are considered. In order to validate the accuracy of the Navier-Stokes solver, solver is tested over a laminar flat plate. The results are compared with analytical solutions. Later, in order to check the performance of the turbulence models, turbulent flow over flat plate and turbulent transonic flow over NACA-0012 airfoil are handled. For turbulent flow over flat plate obtained results are compared with analytical and empirical solutions, whereas for transonic turbulent flow obtained results are compared with numerical and experimental solutions.

Keywords: Navier-Stokes Equations, Finite Volume Method, Finite Difference Method, Spalart-Allmaras Turbulence Model, Baldwin-Barth Turbulence Model.

ÖZ

TÜRBÜLANS MODELLERİNİN BİR NAVIER-STOKES ÇÖZÜCÜSÜNE UYGULANMASI

MUŞTA, Mustafa Nail

Yüksek Lisans, Makina Mühendisliği Bölümü

Tez Yöneticisi: Prof. Dr. M. Haluk Aksel

Eylül 2004, 91 sayfa

Türbülanslı akış problemlerini hesaplamak için, daha önceden geliştirilen Reynolds averajlı, belirli zaman ilerlemeli Navier-Stokes çözücüsüne, tek denklemli türbülans modelleri eklenmiştir. Navier-Stokes denklemlerinin sayısal olarak ayrıştırılması, hücre köşeli sonlu hacim yönteminin tek adımlı uzayda ikinci derecede hassasiyete sahip Lax-Wendroff nümerik yöntemiyle birleşmesine dayanmaktadır. Türbülans viskositesinin hesaplanması için tek denklemli Spalart-Allmaras ve Baldwin-Barth denklemleri kullanılmıştır. Spalart-Allmaras ve Baldwin-Barth denklemlerinin sayısal olarak ayrıştırılması için bu çalışmada Navier-Stokes denklemi için kullanılan sonlu hacim yöntemi ve sonlu farklar sayısal ayrıştırma yöntemi kullanılmıştır.

Çözücünün yakınsama hızını artırmak için yerel zaman adımlama tekniği uygulanmıştır. Sayısal yöntemin sonucu olan salınımları gidermek için ikinci ve dördüncü dereceden yapay sönümlemeler eklenmiştir.

Üç adet test durumu kullanılmıştır. Navier-Stokes çözücüsünün doğruluğunun sağlanması için çözücü düz bir plaka üzerinde laminer bir akış problemi üzerine test edilmiştir. Daha sonra türbülans modellerinin performanslarının test edilmesi için düz bir plaka üzerine türbülanslı akış ve NACA-0012 uçak kanat kesidi üzerine sescivarı türbülanslı akış problemleri ele alınmıştır. Türbülanslı düz bir plaka için elde edilen sonuçlar analitik ve korelasyon sonuçlarıyla karşılaştırılırken, NACA-0012 çözümleri nümerik ve deneysel sonuçlarla karşılaştırılmıştır.

Anahtar Kelimeler: Navier-Stokes Denklemleri, Sonlu Hacim Yöntemi, Sonlu Farklar Yöntemi, Spalart-Allmaras Türbülans Modeli, Baldwin-Barth Türbülans Modeli.

ACKNOWLEDGMENTS

TABLE OF CONTENTS

LIST OF FIGURES

LIST OF SYMBOLS

$\vec{A}$	Surface Vector
A^+	Closure coefficient for a one-equation turbulence model
$A_2{}^+$	Closure coefficient for a one-equation turbulence model
c	Speed of sound
C_{b1}	Closure coefficient for one-equation turbulence model
C_{b2}	Closure coefficient for one-equation turbulence model
C_μ	Closure coefficient for one-equation turbulence model
$C_{\varepsilon1}$	Closure coefficient for a one-equation turbulence model
C_{v1}	Closure coefficient for a one-equation turbulence model
C_{t1}	Closure coefficient for a one-equation turbulence model
C_{t2}	Closure coefficient for a one-equation turbulence model
C_{t3}	Closure coefficient for a one-equation turbulence model
C_{t4}	Closure coefficient for a one-equation turbulence model
C_{w1}	Closure function for a one-equation turbulence model
C_{w2}	Closure coefficient for a one-equation turbulence model
C_{w3}	Closure coefficient for a one-equation turbulence model
E	Total energy per unit volume
F	Inviscid Flux vector in x-direction
f_{t1}	Closure function for a one-equation turbulence model
f_{t2}	Closure function for a one-equation turbulence model
f_{v1}	Closure function for a one-equation turbulence model
f_{v2}	Closure function for a one-equation turbulence model
f_w	Closure function for a one-equation turbulence model
G	Inviscid Flux vector in y-direction
g	Closure function for a one-equation turbulence model
h	Total enthalpy
$\vec{i}$	Unit vector in x-direction
$\vec{j}$	Unit vector in y-direction
J	Jacobian
k	Turbulent kinetic energy
k_R	Average height of a sand-grain
L	Similarity Matrix
M	Mach number

$\vec{n}$	Unit normal vector
p	Static pressure
Pr	Prandtl number
Q	Conservative variable, space coordinate
q	Heat flux
$\vec{r}$	Position vector
R	Universal Gas Constant
r	Closure coefficient for a one-equation turbulence model
Re_T	Turbulent Reynolds number
Re	Reynolds number
$\vec{S}$	Surface vector
S	Magnitude of vorticity
t	Time
T	Temperature
u	Velocity component in x-direction
U	Conservative variable vector
U_e	Boundary layer edge velocity
v	Velocity component in y-direction
$\vec{V}$	Velocity vector
W	Characteristic variable vector
x	Spatial variable in physical domain
y	Spatial variable in physical domain

Greek Symbols

γ	Ratio of specific heats
δ	Correction operator, boundary layer thickness
δ_v^*	Velocity thickness
Δ^2	Second-order change operator
Δt	Time step
$\Delta \forall$	Cell volume
ζ	Local coordinate in computational domain
ε	Dissipation rate of turbulent kinetic energy
η	Local coordinate in computational domain, Blasius similarity variable
κ	Thermal conductivity, closure coefficient for a one-equation model

λ	Eigenvalues of the diagnolized Jacobian matrix
Λ	Diagonalized jacobian matrix
μ	Absolute viscosity
ξ	Local coordinate in computational domain
ρ	Density
σ	Artificial smoothing coefficient ,Closure coefficient for a one-equation turbulence model
σ_ε	Closure coefficient for a one-equation turbulence model
τ	Shear stress
ϕ	Dummy variable
$\bar{\omega}$	Vorticity vector
∇	Gradient operator
∂	Partial derivative operator

Subscripts

corrected	Corrected value
far	Far-field value
i	Node index
inviscid	Inviscid
lam	Laminar
n	Normal direction
predicted	Predicted value
s	Tangential direction
total	Total (Stagnation) value, Total effective value
tur	Turbulent
v	Viscous component of flux vector
viscous	Viscous
wall	Property calculated on the wall
∞	Free stream value

Superscripts

n	Time level
thermal	Thermal conductivity
-	Value known from the previous time step
~	Primitive form
+	Non-dimensional variable

CHAPTER 1

INTRODUCTION

1.1 WHAT IS CFD?

The governing equations of fluid flow problem in macroscale are conservation of mass, conservation of momentum, and the energy equations. These equations form nonlinear partial differential equations (PDE). Because of the nonlinear nature of the problem analytical solutions can be possible only for few cases [1].

In order to include all the physical details of the problem formulation, during the end of 1960' s total numerical simulation stepped in, in such away that it can handle the governing equations in their complete form. Throughout the time it became a popular and reliable tool in engineering analysis. Today numerical (computational) procedures support experiments, enrich the range of analytical solutions and finally contribute in product development [1]. So Computational Fluid Dynamics (CFD) can be described as the art of replacing the differential equations governing the Fluid Flow, with a set of algebraic equations which are obtained by discretizing the governing differential equations, which in turn can be solved with the aid of a computer to get an approximate solution [2].

The rapid increase in the performance of the computers and decrease in the cost of computations compared to the cost of performing experiments has made CFD an alternative. The calculation of aerodynamic characteristics related to any new design through the application of CFD is becoming cheaper than the making the prototype and measuring these characteristics in a wind tunnel. Beside the economical advantages of CFD over experimental studies there are several others, such as reduction of lead times of new designs, ability to study systems where it is difficult or impossible to control experiments and ability to study systems under hazardous conditions. Moreover numerical simulation provides detailed flow field information when required. Even in very reliable experiments, measurements are generally taken at a few points, whereas unlimited level of detail of results can be obtained in CFD [2].

Nowadays, CFD methodologies are not only routinely used for design purposes such as aircraft, turbomachinery, car, and ship design, but also applied in the fields of physical and applied sciences such as meteorology, oceanography, astrophysics, oil recovery and architecture [1]. On the other hand, it should not be thought that CFD represent a mature technology now, since there are many problems in CFD like turbulence and combustion modeling, efficient solution techniques for viscous flows, heat transfer, robust but accurate discretization methods, etc. Also the connections of CFD with other disciplines like structural mechanics require further research. New opportunities arise in the design optimization by using CFD [1].

1. 2. TURBULENCE MODELING FOR CFD

1.2.1 What is Turbulence?

Turbulent flow is the most common type of flow; also the most complicated form of the fluid motion. It is so common that almost all fluid flow which we encounter in daily life is turbulent. Some typical examples are flow around cars, airplanes and buildings. Moreover the flow during the combustion process in engines, in piston engines, gas turbines and combustors are highly turbulent.

Turbulence is that state of fluid motion which is characterized by apparently random and chaotic three-dimensional vorticity. If there is no three-dimensional vorticity, there is no real turbulence [3]. A brief explanation to this is its ability to generate new vorticity from old vorticity that is essential to turbulence and only in a three dimensional flow is the necessary stretching and turning of vorticity by the flow is possible When turbulence is present it usually dominates all other flow phenomena and results in increased energy dissipation, mixing, heat transfer and drag [4].

Although turbulence is defined by Von Karman and G.I.Taylor in 1937, Hinze in 1975 and various other scientists throughout the time [5], there is no exact definition on the turbulent flow, but it has a number of features which are defined below [5, 6]:

I. Irregularity: Turbulent flow is irregular, random and chaotic. Although turbulence is chaotic it is deterministic and it is described by the Navier-Stokes equations.

II. Diffusivity: In turbulent flow the diffusivity increases, which causes rapid mixing of fluids. This means that the spreading rate of boundary layers, jets, etc. increases as the flow becomes turbulent. As the diffusivity increases, the exchange of momentum, heat and mass transfer also increases. Moreover, increased diffusivity also increases the resistance (wall friction) in internal flows such as in channels and pipes.

III. Large Reynolds Numbers: Turbulent flow occurs at high Reynolds number. For instance, the transition to turbulent flow in pipes occurs at $Re_x \cong 2000$, and in boundary layers $Re_d \cong 100000$.

IV. Three Dimensional: Turbulent flow is always three-dimensional. However, when the equations are time averaged one can treat the flow as two-dimensional and if the velocity fluctuations are two dimensional one cannot talk about random vorticity fluctuations which characterize turbulence.

V. Dissipation: Turbulent flow is dissipative, which means that kinetic energy in the small dissipative eddies are transformed into internal energy. As a consequence of the cascade process, dissipation occurs in turbulent flow. In the cascade process, small turbulent scales (eddies) receive their kinetic energy from slightly larger eddies and the slightly larger receive their energy from even larger eddies and the largest eddies extract energy from the mean flow. Turbulence needs a continuous supply of energy. If energy is not supplied, turbulence decays suddenly.

VI. Continuum: Turbulence is a continuum phenomenon, governed by the equations of fluid mechanics. Even though the small turbulent scales in the flow are much larger than the molecular scale, the flow can be treated as continuum.

VII. Turbulence is a feature of fluid flow but not a feature of fluids.

1.2.2 Reasons of Studying Turbulence Modeling:

First of all there is no sufficient information about turbulence to consider engineering problems since there are always fewer equations than unknowns in any attempt to predict anything other than the instantaneous motions. This is known as the famous turbulence closure problem [4].

On the other hand, closure is not a problem with so called Direct Numerical Simulations (DNS). In DNS, three dimensional time dependent Navier-Stokes equations are solved numerically to give an adequately exact description of turbulence. But despite the performance of modern super computers today, DNS is applicable to only simple flow problems. Unfortunately using DNS to engineering problems can be performed if present computers are much more developed and this will take probably too many years [3]. Moreover, the details of unsteady, three dimensional effects of turbulence are not required for design purposes. Time averaged or space averaged (filtered) quantities are appropriate and cost effective. But however it is pity that averaging leads to additional terms, which require semi-empirical models [3, 7].

1.2.3 Turbulence Modeling:

Turbulence models for general-purpose CFD must be frame-invariant i.e. independent of any particular coordinate system-and hence must be expressed in tensor form. This rules out simpler models such as 'boundary-layer type' (e.g. mixing-length models).

Turbulent flows are computed either by solving the Reynolds-averaged Navier-Stokes equations with suitable models for turbulent fluxes or by computing the fluctuating quantities directly. Some of the main approaches are summarized below [6, 8]:

i. Large-eddy simulation (LES)

In LES one can take advantage of the fact that the most of the transport of momentum or thermal energy is carried out by the larger eddies. The small eddies are slightly affected by the boundary conditions of the flow, they are nearly isotopic statistically speaking. They are also weak and do not considerably contribute to turbulent transport. So in LES, large eddies are resolved and statistically simpler subgrid-scale (SGS) eddies are modeled. Obtained solutions in LES are almost as well as DNS, but at as much less computing cost [3].

ii. Reynolds-Averaged Navier-Stokes (RANS) Models

Reynolds averaged Navier-Stokes equations were established by Reynolds in 1895. Reynolds averaging method was the first method for the approximate treatment of turbulent flows. In this method, the Reynolds equations are derived by decomposing the dependent variables in the conservation equations into mean and fluctuating components. The governing equations are then solved for the mean values, which are obtained by an averaging procedure. Reynolds averaging leads to an additional tensor of stresses in momentum equation. These stresses are called the Reynolds stresses. Reynolds stresses are six additional terms in the momentum equations. They characterize the transfer of momentum by turbulence. These are unknowns and must be modeled [7].

1.3. MODELING THE REYNOLDS STRESSES

A satisfactory model must characterize the transfer of momentum by the turbulence but can only do so in terms of the mean flow and mean values of the Reynolds Stresses. This is because averaging removes all information about the turbulent energy cascade and the scales of the turbulence which yield the lost of a huge amount of information about a complex process and limit the applicability of the model. Reynolds Stress modeling can be divided into two. First order models which are algebraic, one and two equation models using the Boussinesq eddy viscosity approximation and Reynolds stress equation models (RSM).

1.3.1 First Order Closure Models:

These models based on the eddy-viscosity hypothesis of Boussinesq approximation.

1.3.2. The Boussinesq Eddy-Viscosity Approximation

The Boussinesq (1877) approximation proposes that the transport of the momentum by the turbulence is a diffusive process and therefore the Reynolds stresses can be modeled using an eddy viscosity, which is analogous to molecular viscosity. The original basis for the approximation is that eddies behaves like molecules. The other assumptions are isotropic turbulence and the local equilibrium between stress and strain. Of course these assumptions are not valid; there are applications for which the Boussinesq hypothesis fails. These cases are listed below [5].

   i. Flows with sudden change of mean strain

   ii. Flows with significant streamline curvature

   iii. Flows with rotation and stratification

iv. Secondary flows in ducts and in turbomachinery

v. Flows with boundary layer separation and reattachment

The limitations of the eddy-viscosity approach are caused by the assumptions of equilibrium between the turbulence and the mean strain field, as well as by the independence on system rotation. The results can be notably improved by using appropriate correction terms in the turbulence models. In order to remove these restrictions imposed by the assumptions of equilibrium between the turbulence and the mean strain rate further non-linear eddy viscosity model is applied.Non-linear eddy viscosity was firstly proposed by Lumley in 1970 which is the extension of the linear Boussinesq approach by higher-order products of strain and rotation tensors. This can be viewed as a Taylor series expansion. Following the Lumley, numerous non-linear eddy viscosity models were proposed.

1.3.3. Type of First Order Models:

First order models deal with the mean equations so second order correlations are modeled. These models based on the eddy-viscosity hypothesis of Boussinesq and according to the number of additional transport equations that are involved by the closure procedure. Once the eddy viscosity constant μ_t is known, Navier-Stokes can easily be extended to simulate turbulent flow by introducing averaged variable and by adding μ_t to the laminar viscosity, which is also what is done in this study. These models can be divided in to three [5]:

i. Zero equation (algebraic closure) models,

ii. One Equation Models,

iii. Two Equation Models.

Zero equation models (algebraic models): Prandtl (1925) introduced the mixing length which was in agreement with the eddy viscosity concept Van Dierst

(1956) improved the mixing length model which become a basis to all algebraic models used today. Cebeci and Smith (1974) refined the eddy-viscosity -mixing-length and established well known Cebeci-Smith model. Baldwin and Lomax (1978) proposed an alternative albegraic model which removed the necessity of defining boundary layer thickness. Since this model is more robust model than the Cebeci-Smith model, it was widely used for many years [5].

One equation models: The first successful one equation model was formulated by Bradshaw, Ferris and Atwell (1967). Most of the older models solved an equation for the turbulent kinetic energy (or the turbulent shear stress), but like the algebraic models, depend on the specification of an algebraic length scale. One equation models were formulated which were based on rather than then kinetic energy. Nee-Kovasznay (1968) formulated a transport equation which solves kinematic eddy viscosity but still it needs a length scale. More recently, Baldwin and Barth (1990), Goldberg (1991) and Spalart and Allmaras (1992) postulated transport equation based on the eddy viscosity. These more recent works were motivated primarily by the ease with which such model equations can be solved numerically, relative to two equation models and stress transport models [5].

Two Equation models: Kolmogorov (1941) proposed the first two equation model of turbulence. Kolmogorov chose the kinetic energy of the turbulence k and the dissipation per unit turbulence kinetic energy, ω as his turbulence parameters. Details about this model can be found in Wilcox [10]. The k-ε model is the most widely used and most validated two equation model today. The parameter ε is a turbulence dissipation rate. This model is first proposed by Harlow and Nakayama (1968). This study was followed by the papers of Launder (1972) and Launder and Spalding (1974). This model has been utilized and improved by many other researchers. One can refer to Wilcox [5] for more information.

1.3.4. Reynolds Stress Equation Models:

Reynolds stress equation models are the most complex classical turbulence model, which are also called the second order or second moment closure model. In these models the exact Reynolds stress transport equation are modeled term by term which result in a set of PDE's for the Reynolds stresses. Then these sets of PDE's are solved with the Reynolds-averaged momentum equations and continuity equation. After sufficient computer resources became available in 1970's, the most significant contributions to this model were made by Donaldson and Rosenbaum (1968), Daly and Harlow (1970) and Lounder, Reece and Rodi (1975). The more recent contributions made by Lumley (1978), Speziale (1985, 1987, 1991) and Reynolds (1987) added mathematical contribution to the closure process. Since these models do not rely on the eddy-viscosity concept, they have given very accurate calculation of mean flow properties and all Reynolds stresses for many simple and more complex flows such as wall jets, asymmetric channel and non circular duct flows and curved flows. However because of computing costs (seven extra PDE's), their complexity and not validated as the other RANS models, they have found very limited number of applications.

Algebraic Stress Models: These models are a simplification of RSM's and emerge as a two equation models with anisotropic eddy-viscosity. The idea of simplification of RSM's firstly proposed by Rodi (1976) and various studies have been made since then. These models are cheaper to account for Reynolds stress anisotropy and successfully applied to isothermal and buoyant thin shear layers. On the other hand they, have not been validated widely and shown good performance to very restricted flows because of the simplifications made.

1.4. PRESENT STUDY

In the present thesis Spalart-Allmaras and Baldwin-Barth one equation turbulence models have been implemented into a previously developed Navier-Stokes solver.

Baldwin-Barth [9, 10, and 11] turbulence model was developed in 1990. This model is derived from standard k-ε two equation model in a procedure of combining standard k-ε model to provide a single equation model in terms of turbulence Reynolds number.

Other one equation turbulence model, which is the Spalart-Allmaras [12] turbulence model, was developed in 1992. Model has similarities with the other one equation models of Nee and Kovasznay, Secundov et all, and Baldwin-Barth. The model is based on kinematic eddy viscosity and it is powerful enough to be calibrated on 2-D mixing layers, wakes and flat-plate boundary layers [12]. Later on Edwards and Chandra made modifications on Spalart-Allmaras turbulence model [13]. The modified Spalart-Allmaras model allows smooth, rapid convergence while retaining the near wall accuracy of the original formulation.

The method used to solve Navier -Stokes equations in this study is one step Ni [14] type Lax-Wendroff scheme , which is second order accurate in space and explicit finite volume method. The discretization method used for Navier Stokes equations in this study is cell-vertex for inviscid and cell-centered for viscous terms. For the turbulence closure equations both finite difference method [11] and Ni [14] type Lax-Wendroff methods are used.

In order to damp numerical oscillations, artificial viscosity terms are added to the equations which are discretized by Lax-Wendroff method. For stability artificial viscosity coefficient is applied higher to the turbulence transport equations than to the Navier -Stokes equations. Moreover same time stepping is used both for turbulence and Navier- Stokes equations.

The outline of the thesis is as follows: Chapter 2 describes the governing equations of the flow that is Navier-Stokes equations and turbulence closure models. Chapter 3 covers the method of discretization, which is based on the type of formulations used by Ni [14] and finite difference discretization of the turbulence models. Artificial viscosity, time stepping terms and calculation of viscous and heat conduction terms are also explained in this chapter. Chapter 4 explains the initial and boundary conditions which are used in this study. Chapter 5 gives the results

obtained for the test cases and discusses them. Finally Chapter 6 presents the summary of the work and conclusions with future recommendations about this work.

CHAPTER 2

GOVERNING EQUATIONS

In this study the governing Navier-Stokes equations are considered for viscid, heat-conducting and compressible flows with respect to the stationary reference frame. It is also assumed that flows are under no external or body force and no heat generation occurs within the flows. In order to close the system of equations perfect gas relations are assumed. Auxiliary relations are used for the calculation of viscosity and conductivity. To calculate the laminar viscosity Sutherland's law of viscosity is used and for the turbulent viscosity one equation turbulence models are used.

The Navier-Stokes equations implemented in the numerical scheme of the thesis are two-dimensional and conservative form in a Cartesian coordinate system. Details about these equations and auxiliary relations are presented below.

2.1. NAVIER-STOKES EQUATIONS

The compressible Navier-Stokes equations are written in a vectorial form as follows:

$$\frac{\partial U}{\partial t} + \frac{\partial F}{\partial x} + \frac{\partial G}{\partial y} = \frac{\partial F_v}{\partial x} + \frac{\partial G_v}{\partial y} + S \qquad (2.1)$$

where

$$U = \begin{bmatrix} \rho \\ \rho u \\ \rho v \\ e \end{bmatrix} \qquad (2.2)$$

$$F = \begin{bmatrix} \rho u \\ \rho u^2 + p \\ \rho u v \\ \rho u h \end{bmatrix} \qquad (2.3a)$$

$$G = \begin{bmatrix} \rho v \\ \rho u v \\ \rho v^2 + p \\ \rho v h \end{bmatrix} \qquad (2.3b)$$

$$F_v = \begin{bmatrix} 0 \\ \tau_{xx} \\ \tau_{xy} \\ \tau_{xx} u + \tau_{xy} v - q_x \end{bmatrix} \qquad (2.3c)$$

$$G_v = \begin{bmatrix} 0 \\ \tau_{yx} \\ \tau_{yy} \\ \tau_{yx} u + \tau_{yy} v - q_y \end{bmatrix} \qquad (2.3d)$$

$$S = \begin{bmatrix} 0 & 0 & 0 & 0 & 0 \end{bmatrix}^T \qquad\qquad (2.3e)$$

where, the total stresses, τ, given by Stokes law of viscosity can be expressed as:

$$\tau_{xx} = \mu_{total}\left(\frac{4}{3}\frac{\partial u}{\partial x} - \frac{2}{3}\frac{\partial v}{\partial y}\right)$$

$$\tau_{yy} = \mu_{total}\left(\frac{4}{3}\frac{\partial v}{\partial y} - \frac{2}{3}\frac{\partial u}{\partial x}\right) \qquad\qquad (2.4)$$

and

$$\tau_{xy} = \tau_{yx} = \mu_{total}\left(\frac{\partial u}{\partial y} + \frac{\partial v}{\partial x}\right)$$

where u and v are the velocity components in the x and y directions, respectively, ρ is the density, p is the static pressure and μ_{total} is the total effective viscosity (sum of the laminar and turbulent viscosities).

Using the equation of state, pressure can be written in terms of the conservative variable as:

$$p = (\gamma - 1)\left(e - \frac{1}{2\rho}\left[(\rho u)^2 + (\rho v)^2\right]\right) \qquad\qquad (2.5)$$

where e is the total internal energy per unit volume. The total enthalpy per unit mass, h is defined as:

$$h = \frac{(e + p)}{\rho} \qquad (2.6)$$

The total heat fluxes given by

$$q_x = -k^{thermal} \frac{\partial T}{\partial x}$$
$$q_y = -k^{thermal} \frac{\partial T}{\partial y} \qquad (2.7)$$

where $k^{thermal}$ is the total thermal conductivity and T stands for the temperature

A dimensionless parameter that is used is the Prandtl number given as follows:

$$P_r = \frac{\mu c_p}{k^{thermal}} \qquad (2.8)$$

while another dimensionless parameter known as the Reynolds number is used in the formulation and is given by

$$Re = \frac{\rho_{ref} l_{ref} a_{ref}}{\mu_{ref}} \qquad (2.9)$$

where the subscript *ref* in the above equation stands for the reference quantities. ρ_{ref}, a_{ref}, μ_{ref}, are set at free stream values. The above equations are completed with the following relations

$$c_p = \frac{\gamma R}{\gamma - 1} \qquad (2.10)$$

and the speed of sound, a

$$a = \sqrt{\gamma R T}$$

<div align="right">(2.11)</div>

where R stands for the gas constant of the fluid and γ stands for the specific heat ratio .

2.2. THERMAL CONDUCTIVITY AND COEFFICIENT OF VISCOSITY

The total effective viscosity μ_{total} is composed of two parts. The laminar as well as the turbulent viscosities are added together based on the Boussinesq eddy-viscosity approximation.

$$\mu_{total} = \mu_{lam} + \mu_{tur}$$

<div align="right">(2.12)</div>

Reynolds proposed a similar assumption and hence, forming the total effective conductivity is based on the addition of turbulent and laminar thermal conductivities given as:

$$k_{total}^{thermal} = k_{lam}^{thermal} + k_{tur}^{thermal}$$

<div align="right">(2.13)</div>

where

$$k_{lam}^{thermal} = \left(\frac{\mu_{lam}}{\Pr_{lam}} \right) \frac{\gamma R}{\gamma - 1}$$

<div align="right">(2.14a)</div>

$$k_{tur}^{thermal} = \left(\frac{\mu_{tur}}{\Pr_{tur}} \right) \frac{\gamma R}{\gamma - 1}$$

<div align="right">(2.14b)</div>

where the subscripts *lam* and *tur* stand for laminar and turbulent flows, respectively. Furthermore, the Prandtl numbers used are constants for both laminar and turbulent cases and they are set depending on the flow in consideration.

2.2.1 Calculation of the Laminar Viscosity

The dynamic viscosity of air is assumed to be a function of temperature only, following Sutherland's law.

$$\mu_{lam} = 1.45x10^{-6} \frac{T^{\frac{3}{2}}}{T + 110.0} \qquad (2.15)$$

In the above equation, temperature is in Kelvin and dynamic viscosity is calculated in units of Pa.s.

2.3 CALCULATION OF TURBULENT VISCOSITY

2.3.1 Spalart and Allmaras Turbulence Model:

The model proposed by the Spalart and Allmaras solves a transport equation for a quantity, which is the modified form of the turbulent kinetic viscosity. The governing equation is derived by using empiricism, dimensional analysis, Galilean invariance and selected dependence on the molecular viscosity. The Spalart-Allmaras model is compatible with any type of grid structure and 2-D or 3-D Navier-Stokes solver. The model includes eight closure coefficients and three closure functions [12].

The transported variable in the Spalart-Allmaras model, $\tilde{v}$ which is a modified version of kinematics viscosity, is identical to the kinematic viscosity except in the near wall (viscous-affected) region. It can be written in tensor form as follows [11].

$$\frac{\partial \tilde{v}}{\partial t} + u_i \frac{\partial \tilde{v}}{\partial x_i} = C_{b1} \tilde{S} \tilde{v} (1 - f_{t2}) + \frac{1}{\sigma_v} \left[\frac{\partial}{\partial x_j} \left\{ (v + \tilde{v}) \frac{\partial \tilde{v}}{\partial x_j} \right\} \right] + \frac{C_{b2}}{\sigma_v} \left(\frac{\partial \tilde{v}}{\partial x_j} \right)^2$$

$$- C_{w1} f_w (1 - f_{t2}) \frac{C_{b1}}{\kappa^2} \left(\frac{\tilde{v}}{d} \right)^2 + f_{t1} \Delta U^2 \qquad (2.16)$$

In above equation, the left-hand side represents advection term while the terms on the right-hand side represent production, diffusion, non-conservative diffusion, destruction and the trip term respectively.

Modeling of the Turbulent Viscosity:

The turbulent viscosity, μ_t is computed from

$$\mu_t = \rho \tilde{v} f_{v1} \qquad (2.17)$$

where the viscous damping function f_{v1} is given by

$$f_{v1} = \frac{X^3}{X^3 + C_{v1}^3} \qquad (2.18a)$$

and

$$X = \frac{\tilde{v}}{v} \qquad (2.18b)$$

Modeling of the Turbulent Production:

The production term is modeled as

$$C_{b1}\tilde{S}\tilde{v}(1-f_{t2})$$
(2.19)

where

$$\tilde{S} = Sf_{v3} + \frac{\tilde{v}}{\kappa^2 d^2}f_{v2}$$
(2.19a)

$$f_{v2} = (1 + \frac{X}{C_{v2}})^{-3}$$
(2.19b)

$$f_{v3} = \frac{(1+Xf_{v1})(1-f_{v2})}{\max(X,0.001)}$$
(2.19c)

and

$$f_{t2} = c_{t3}\exp(-c_{t4}X^2)$$
(2.19d)

in the above equations C_{b1}, C_{t4}, C_{t3} and κ are constants, d is the distance from the wall and S is a scalar measure of the deformation tensor.

$$S = \sqrt{2\Omega_{ij}\Omega_{ij}}$$
(2.19e)

where Ω_{ij} is the mean rate of rotation tensor and is defined by

$$\Omega_{ij} = \frac{1}{2}\left(\frac{\partial u_i}{\partial x_j} - \frac{\partial u_j}{\partial x_i}\right) \tag{2.20f}$$

The justification for the default expression for S is that, for the wall-bounded flows that were of most interest when the model was formulated, turbulence is found only where vorticity is generated near walls. However, it has been acknowledged that one should also take in to account the effect of mean strain on the turbulence production, and a modification to the model has been proposed by the Dacles [23]. This modification combines measures of both rotation and strain tensors in the definition of S.

$$S = \left|\Omega_{ij}\right| + C_{prod}\,\min\left(0, \left|S_{ij}\right| - \left|\Omega_{ij}\right|\right) \tag{2.20g}$$

where $C_{prod} = 2.0$, $\left|\Omega_{ij}\right| = \sqrt{2\Omega_{ij}\Omega_{ij}}$ and $\left|S_{ij}\right| = \sqrt{2S_{ij}S_{ij}}$ with the mean strain rate, S_{ij} is defined as

$$S_{ij} = \frac{1}{2}\left(\frac{\partial u_i}{\partial x_j} + \frac{\partial u_j}{\partial x_i}\right) \tag{2.20h}$$

In the original version, $\widetilde{S}$ was defined in such a way that it could become negative. But this could disturb the value of r and stall convergence. So the function f_{v3} is introduced and the definition of the function f_{v2} has been changed. This modification was suggested by Spalart in order to prevent $\widetilde{S}$ from being negative [1].

Modeling of the Turbulent Destruction:

The destruction term is modeled as follows:

$$C_{w1} f_w (1 - f_{t2}) \frac{C_{b1}}{\kappa^2} \left(\frac{\tilde{v}}{d} \right)^2 \qquad (2.21a)$$

with

$$f_w(r) = g \left[\frac{1 + C_{w3}^{\ 6}}{g^6 + C_{w3}^{\ 6}} \right]^{1/6} \qquad (2.21b)$$

$$g = r + C_{w2}(r^6 - r) \qquad (2.21c)$$

$$r = \frac{\tilde{v}}{\tilde{S} \kappa^2 d^2} \qquad (2.21d)$$

where C_{w1}, C_{w2} and C_{w3} are constants and large values of r should be truncated to a value about 10.

Modeling of the Trip term:

This term allows one to specify explicitly the boundary layer transition location and which is

$$\rho f_{t1} \Delta U^{\ 2} \qquad (2.22)$$

where

$$f_{t1} = c_{t1} g_t \exp(-c_{t2} \frac{w_t^{\ 2}}{\Delta U^{\ 2}} (d^2 + g_t^{\ 2} d_t^{\ 2})) \qquad (2.23)$$

where d_t is the distance to the nearest trip point, w_t is the vorticity at the wall at the trip point, ΔU is the norm of the difference between the velocity at the trip point

(zero if the wall stationary) and $g_t = \min(0.1, \Delta U / \omega_t \Delta x)$ where Δx is the spacing along the wall at the trip point.

Although the model allows the transition point localization, all the computed flow fields are assumed to be fully turbulent in this work when the Spalart-Allmaras model is used. Hence, this term is not used.

Model Constants

The model constants $C_{b1}, C_{b2}, \sigma_{\tilde{v}}, C_{v1}, C_{w1}, C_{w2}, C_{w3}$, Ct_{t3}, C_{t4}, and κ have the following default values.

C_{b1}=0.1355, $C_{b2,}$=0.622, σ_v=2/3, C_{v1}=7.1, C_{w2}=0.3, κ=0.4187

C_{t4}=2, $C_{t3,}$=1.1, C_{t2}=2, $C_{t1,}$=1. and

$$C_{w1} = \frac{C_{b1}}{\kappa^2} + \frac{(1 + C_{b2}}{\sigma_{\tilde{v}}} \tag{2.24}$$

2.3.2 Spalart-Allmaras Equation in Vectorial Form

Spalart-Allmaras equation in Equation (2.16) can also be written in vectorial form. If Equation (2.18) is multiplied by density ρ, Spalart-Allmaras equation can be represented in conservative form .This form of Spalart-Allmaras equation can easily be descritized and coupled with Navier-Stokes equations [1].

$$\frac{\partial U_{tur}}{\partial t} + \frac{\partial F_{tur}}{\partial x} + \frac{\partial G_{tur}}{\partial y} = S_{tur} \tag{2.25}$$

where

$$U_{tur} = \left[\rho\tilde{v}\right] \tag{2.26a}$$

$$F_{tur} = \left[\rho u\tilde{v} - \left(\frac{1}{\sigma_v}(\mu_{lam} + \rho\tilde{v})\right)\frac{\partial\tilde{v}}{\partial x}\right] \tag{2.26b}$$

$$G_{tur} = \left[\rho v\tilde{v} - \left(\frac{1}{\sigma_v}(\mu_{lam} + \rho\tilde{v})\right)\frac{\partial\tilde{v}}{\partial y}\right] \tag{2.26c}$$

$$S_{tur} = \left[C_{b1}\rho(1-f_{t2})\tilde{S}\tilde{v} + \frac{C_{b2}\rho}{\sigma_v}\left[\left(\frac{\partial\tilde{v}}{\partial x}\right)^2 + \left(\frac{\partial\tilde{v}}{\partial y}\right)^2\right] - \left[C_{W1}f_w\rho - \frac{C_{b1}\rho}{\kappa^2}f_{t2}\right]\left(\frac{\tilde{v}}{d}\right)^2 + \rho f_{t1}\Delta U^2\right]$$

$$(2.26d)$$

2.4   Baldwin Barth Turbulence Model:

The Baldwin-Barth one equation model is obtained from the standard two equation k-ε model in terms of the turbulent Reynolds number $Re_T = k^2/v\varepsilon$. The variables in the turbulent Reynolds number, which are k, ε and v stand for turbulent kinetic energy, dissipation of turbulence and kinematic viscosity, respectively [9, 10 and 11].

$$\frac{\partial(v\overline{\mathrm{Re}}_T)}{\partial t} + u_i\frac{\partial v\overline{\mathrm{Re}}_T}{\partial x_i} = (C_{\varepsilon 2}f_2 - C_{\varepsilon 1})\sqrt{v\,\overline{\mathrm{Re}}_T}\,P + (v + \frac{v_t}{\sigma_\varepsilon})\nabla^2(v\overline{\mathrm{Re}}_T)$$

$$-\frac{1}{\sigma_\varepsilon}(\nabla v_t).(\nabla(v\overline{\mathrm{Re}}_T)) \tag{2.27}$$

In the above equation the left-hand side represents advection term, while the terms on the right-hand side represent production, diffusion and the destruction term respectively.

Modeling of the Turbulent Viscosity:

The turbulent viscosity, μ_t is computed from

$$\mu_t = C_\mu (v\overline{R}_T) D_1 D_2 \, \rho \qquad (2.28a)$$

where D_1 and D_2 are the viscous damping functions which extend the validity of the model to near-wall regions. These terms are given as

$$D_1 = 1 - \exp(-y^+ / A^+) \qquad (2.28b)$$

and

$$D_2 = 1 - \exp(-y^+ / A_2^+) \qquad (2.28c)$$

where y^+ is the non-dimensional wall distance calculated as

$$y^+ = \frac{\rho}{\mu_{lam}} u_\tau . y \qquad (2.28d)$$

and u_τ is the friction velocity defined as follows:

$$u_\tau = \sqrt{\frac{\tau_{wall}}{\rho}} \qquad (2.28e)$$

Modeling of the Turbulent Production:

The production term is based on Boussinesq assumption and modeled as follows

$$(C_{\varepsilon 2} f_2 - C_{\varepsilon 1})\sqrt{\nu \, \overline{\overline{Re}}_t \, P} \qquad (2.29a)$$

where

$$P = \nu_t \left(\frac{\partial u_i}{\partial x_j} + \frac{\partial u_j}{\partial x_i} \right) \frac{\partial u_i}{\partial x_j} - \frac{2}{3}\nu_t \left(\frac{\partial u_k}{\partial x_k} \right)^2 = \nu_t S^2 \qquad (2.28b)$$

$$f_2(y^+) = \frac{C_{\varepsilon 1}}{C_{\varepsilon 2}} + \left(1 - \frac{C_{\varepsilon 1}}{C_{\varepsilon 2}} \right) \left[\frac{1}{\kappa y^+} + D_1 D_2 \right] \left[\sqrt{D_1 D_2} + \frac{y^+}{\sqrt{D_1 D_2}} \right.$$

$$\left. \left(\frac{1}{A^+} \exp(-y^+/A^+) D_2 + \frac{1}{A_2^+} \exp(-y^+/A_2^+) D_1 \right) \right]$$

$$(2.28c)$$

using Equation (2.28a) and (2.28b) production term can be written as follows

$$(C_{\varepsilon 2} f_2 - C_{\varepsilon 1})\sqrt{C_\mu D_1 D_2} \, S \nu \, \overline{\overline{Re}}_t \qquad (2.28d)$$

Modeling of the Turbulent Destruction:

The destruction term is given as follows

$$\frac{1}{\sigma_\varepsilon}(\nabla \nu_t).(\nabla(\nu \, \overline{\overline{Re}}_T) \qquad (2.29a)$$

where

$$\sigma_\varepsilon = \left(\frac{\kappa^2}{(C_{\varepsilon_2} - C_{\varepsilon_1})\sqrt{C_\mu}} \right) \qquad (2.29b)$$

same function σ_ε is also used in the diffusion term, so all the terms are already defined for the diffusion term.

Model Constants

The model constants $C_{\varepsilon 1}, C_{\varepsilon 2}, C_\mu, \kappa, A^+$ and A_2^+ have the following default values:

$C_{\varepsilon 1} = 1.2,\ C_{\varepsilon 2,} = 2.0,\ \kappa = 0.4187,$

$$(2.30)$$

$C_\mu = 0.04,\ A^+ = 26 \text{ and } A_2^+ = 10$

For the ease of discretization, destruction and diffusion terms are modified which is suggested by Hoffman [11], as result final form of the Equation (2.26) is given as follows

$$\frac{\partial(v\,\overline{\mathrm{Re}}_T)}{\partial t} + u_i \frac{\partial v\,\overline{\mathrm{Re}}_T}{\partial x_i} = (C_{\varepsilon 2} f_2 - C_{\varepsilon 1})\sqrt{C_\mu D_1 D_2}\, Sv\,\overline{\mathrm{Re}}_t + (v + \frac{v_t}{\sigma_\varepsilon})\nabla^2(v\,\overline{\mathrm{Re}}_T)$$

$$- \frac{1}{\sigma_\varepsilon}\nabla.v_t \nabla(v\,\overline{\mathrm{Re}}_T) \qquad (2.31)$$

CHAPTER 3

SOLUTION METHOD

In this chapter, mainly numerical techniques used for the discretization of Navier-Stokes equations and turbulence closure equations are presented. For the discretization of Navier-stokes equations coupled with Spalart-Allmaras turbulence model, Ni's [14] scheme is used. Spalart-Allmaras turbulence model is also discretised by finite difference method besides the Baldwin-Barth turbulence model. Details about implementation procedures of these numerical methods are discussed in this chapter. Moreover, formulations of the time stepping terms and artificial smoothing terms are also presented.

3.1. DISCRETIZATION METHOD

The discretization technique used for the Navier-Stokes equations coupled with Spalart-Allmaras equation is an explicit finite volume method. In the application process of this method, for the inviscid and source terms first order approach; and for the viscous terms and second order inviscid terms cell centered approach is used. This technique is based on a one-step Lax-Wendroff scheme. It was firstly introduced by Ni [14] for the solution of Euler equations and later improved to solve for Navier-Stokes equations [15, 16]. The derivation of the scheme starts with the second order Taylor series expansion of the time derivatives.

$$U^{n+1} = U^n + \Delta t \left(\frac{\partial U}{\partial t} \right)^n + \frac{\Delta t^2}{2} \left(\frac{\partial^2 U}{\partial t^2} \right)^n \qquad (3.1)$$

where U is the conservative variable vector and the superscript n denotes the time step. By using equation (2.1), the term $\dfrac{\partial U}{\partial t}$ can be defined as below

$$\frac{\partial U}{\partial t} = -\frac{\partial F}{\partial x} - \frac{\partial G}{\partial y} + \frac{\partial F_v}{\partial x} + \frac{\partial G_v}{\partial y} + S \qquad (3.2)$$

Inserting Equation (3.2) into Equation (3.1) and define the change term; residual $\delta U = U^{n+1} - U^{n}$; one can obtain

$$\delta U = U_i^{n+1} - U_i^{n} = -\Delta t\left(\frac{\partial F}{\partial x} + \frac{\partial G}{\partial y}\right)^{n} + \Delta t\left(\frac{\partial F_v}{\partial x} + \frac{\partial G_v}{\partial y}\right)^{n} + \Delta t(S)^{n}$$

$$-\frac{\Delta t^2}{2}\frac{\partial}{\partial t}\left(\frac{\partial F}{\partial x} + \frac{\partial G}{\partial y}\right)^{n} + \frac{\Delta t^2}{2}\frac{\partial}{\partial t}\left(\frac{\partial F_v}{\partial x} + \frac{\partial G_v}{\partial y}\right)^{n} + \frac{\Delta t^2}{2}\frac{\partial}{\partial t}(S)^{n} \qquad (3.3)$$

The second order viscous and the source terms are generally neglected, due to the fact that they have negligible effect on the convergence history and final solution [16, 17, and 18]. Besides this fact, the terms on the right hand sight of the Equation (3.3) are known and stand for the same time level, so the superscript n can be removed from this equation. With these considerations, Equation (3.3) becomes

$$\delta U = -\Delta t\left(\frac{\partial F}{\partial x} + \frac{\partial G}{\partial y}\right) + \Delta t\left(\frac{\partial F_v}{\partial x} + \frac{\partial G_v}{\partial y}\right) + \Delta t(S) - \frac{\Delta t^2}{2}\frac{\partial}{\partial t}\left(\frac{\partial F}{\partial x} + \frac{\partial G}{\partial y}\right)$$

$$(3.4)$$

the last term in the above equation is the second order inviscid flux term; it can be rearranged as below:

$$\frac{\Delta t^2}{2} \cdot \frac{\partial}{\partial t}\left(\frac{\partial F}{\partial x} + \frac{\partial G}{\partial y}\right) = \frac{\Delta t^2}{2}\left[\frac{\partial}{\partial x}\left(\frac{\partial F}{\partial t}\right) + \frac{\partial}{\partial y}\left(\frac{\partial G}{\partial t}\right)\right]$$

$$= \frac{\Delta t^2}{2}\left[\frac{\partial}{\partial x}\left(\frac{\partial F}{\partial U}\frac{\partial U}{\partial t}\right) + \frac{\partial}{\partial y}\left(\frac{\partial G}{\partial U}\frac{\partial U}{\partial t}\right)\right]$$

$$= \frac{\Delta t}{2}\left[\frac{\partial}{\partial x}\left(\frac{\partial F}{\partial U}\frac{\partial U}{\partial t}\Delta t\right) + \frac{\partial}{\partial y}\left(\frac{\partial G}{\partial U}\frac{\partial U}{\partial t}\Delta t\right)\right] \qquad (3.5)$$

$$= \frac{\Delta t}{2}\left[\frac{\partial}{\partial x}\left(\frac{\partial F}{\partial U}\Delta U\right) + \frac{\partial}{\partial y}\left(\frac{\partial G}{\partial U}\Delta U\right)\right]$$

where,

$$\Delta U = \frac{\partial U}{\partial t}\Delta t \qquad (3.6)$$

also Jacobians of the inviscid flux vectors can be written as below [14].

$$\Delta F = \frac{\partial F}{\partial U}\Delta U$$

$$\qquad (3.7)$$

$$\Delta G = \frac{\partial G}{\partial U}\Delta U$$

Substituting these definitions into Equation (3.2) one can obtain

$$\delta U = -\Delta t\left(\frac{\partial F}{\partial x} + \frac{\partial G}{\partial y}\right) + \Delta t\left(\frac{\partial F_v}{\partial x} + \frac{\partial G_v}{\partial y}\right) + \Delta t S - \frac{\Delta t}{2}\left(\frac{\partial(\Delta F)}{\partial x} + \frac{\partial(\Delta G)}{\partial y}\right) \qquad (3.8)$$

The change of ΔU and Jacobians of inviscid fluxes can be expressed as follows Ni [14]:

$$\Delta U = \begin{bmatrix} \Delta\rho \\ \Delta(\rho u) \\ \Delta(\rho v) \\ \Delta e \\ \Delta(\rho\tilde{v}) \end{bmatrix} \tag{3.9a}$$

$$\Delta F = \left(\frac{\partial F}{\partial U}\right)\Delta U = \begin{bmatrix} \Delta(\rho u) \\ u\Delta(\rho u) + \rho u\Delta u + \Delta p \\ v\Delta(\rho u) + \rho u\Delta v \\ h\Delta(\rho u) + \rho u\Delta h \\ \tilde{v}\Delta(\rho u) + u\Delta(\rho\tilde{v}) - u\tilde{v}\Delta\rho \end{bmatrix} \tag{3.9b}$$

$$\Delta G = \left(\frac{\partial G}{\partial U}\right)\Delta U = \begin{bmatrix} \Delta(\rho v) \\ u\Delta(\rho v) + (\rho v)\Delta u \\ v\Delta(\rho v) + (\rho v)\Delta v + \Delta p \\ h\Delta(\rho v) + (\rho v)\Delta h \\ \tilde{v}\Delta(\rho v) + v\Delta(\rho\tilde{v}) - (v\tilde{v})\Delta\rho \end{bmatrix} \tag{3.9c}$$

All the terms in ΔF and ΔG can be expressed by the terms in ΔU by using following relations.

$$\Delta u = \frac{1}{\rho}[\Delta(\rho u) - u\Delta\rho]$$

$$\Delta v = \frac{1}{\rho}[\Delta(\rho v) - v\Delta\rho]$$

$$\Delta p = (\gamma - 1)\left[\Delta e - \frac{1}{2}(u\Delta(\rho u) + v\Delta(\rho v) + \rho u\Delta u + \rho v\Delta v)\right] \tag{3.10}$$

$$\Delta h = \frac{1}{\rho}[\Delta e + \Delta p - h\Delta\rho]$$

In order to understand the finite volume integration procedure better, it is better to define the mesh structure of a typical cell,
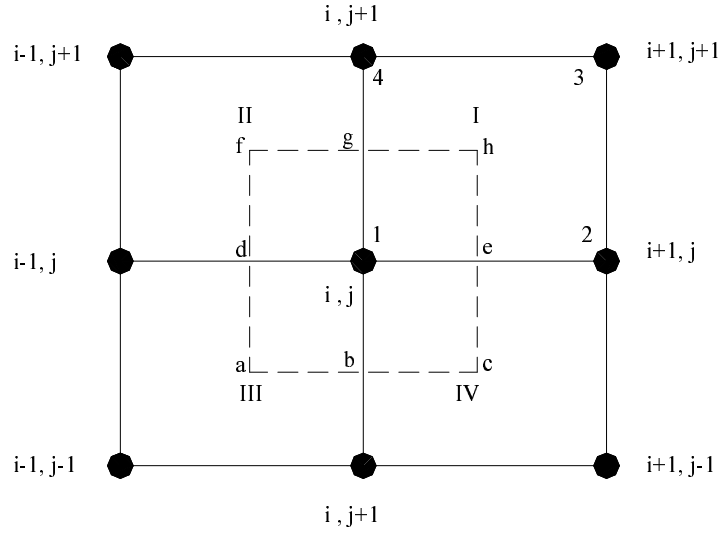
Figure 3.1 Mesh structure around node 1

as shown for particular node 1 in Figure 3.1. There are two types of control volumes. The primary one is represented by the thick lines and formed by joining the cell nodes; and the transformed one is represented by dashed lines and formed by joining the cell centers of the four surrounding cells of node 1. The primary control volume is used to calculate the first order inviscid terms and the source terms. On the other hand transformed control volume is used to handle the second order source terms and viscous terms.

Integrating form of Equation (3.8) over control volumes, one can obtain

$$\int_{\delta\forall} \delta U \mathrm{d}\forall = -\int_{\delta\forall} \Delta t \left(\frac{\partial F}{\partial x} + \frac{\partial G}{\partial y} \right) \mathrm{d}\forall + \int_{\delta\forall} \Delta t \left(\frac{\partial F_v}{\partial x} + \frac{\partial G_v}{\partial y} \right) \mathrm{d}\forall + \int_{\delta\forall} (\Delta t S) \mathrm{d}\forall$$

$$- \int_{\delta\forall} \frac{\Delta t}{2} \left(\frac{\partial(\Delta F)}{\partial x} + \frac{\partial(\Delta G)}{\partial y} \right) \mathrm{d}\forall \qquad (3.11)$$

where $\mathrm{d}\forall$ is the volume of the control volume surrounding a particular node.

31

In order to calculate the total contribution of the changes on node 1, Equation (3.11) can be split into four equations. These equations are the integral equations of the four portions of the control volumes within the cells of numbered I-II-III and IV. So, the summation of the contributions from the surrounding four cells can be written as below.

$$\delta U_1 = \delta U_{1I} + \delta U_{1II} + \delta U_{1III} + \delta U_{1IV} \tag{3.12}$$

In Equation (3.12), δU_{1I} stands for the part of the contribution of the change in cell I into node 1 and can be expressed as follows:

$$\delta U_{1I} = -\frac{1}{4}\frac{\Delta t}{\Delta\nabla_I}\int_{cell-I}\left(\frac{\partial F}{\partial x} + \frac{\partial G}{\partial y}\right)d\nabla + \frac{1}{4}\frac{\Delta t}{\Delta\nabla_I}\int_{cell-I}Sd\nabla$$

$$+\frac{\Delta t}{\Delta\nabla_I}\int_{1ehg}\left(\frac{\partial F_x}{\partial x} + \frac{\partial G_y}{\partial y}\right)d\nabla - \frac{\Delta t}{2\Delta\nabla_I}\int_{1ehg}\left(\frac{\partial(\Delta F)}{\partial x} + \frac{\partial(\Delta G)}{\partial y}\right)d\nabla \tag{3.13}$$

In the above equation, in front of the first and second integrals, which are the first order inviscid term and source term respectively, there is coefficient of ¼. This is due to the equal distribution of the total change of cell I among its nodes. On the other hand, the third and fourth integrals, which are first order viscous and second order inviscid fluxes respectively, don't have this coefficient of 1/4 since these integrals are evaluated on the one-fourth of the transformed control volume.

By using Gauss' divergence theorem, the volume integrals in Equation (3.13) can be converted into area integrals as follows

$$\delta U_{1I} = -\frac{1}{4}\frac{\Delta t}{\Delta\nabla_I}\int_{cell-I}\left(FdS_x + GdS_y\right) + \frac{1}{4}\frac{\Delta t}{\Delta\nabla_I}\int_{cell-I}Sd\nabla$$

$$+\frac{\Delta t}{\Delta\nabla_I}\int_{1ehg}\left(F_v dS_x + G_v dS_y\right) - \frac{\Delta t}{2\Delta\nabla_I}\int_{1ehg}\left(\Delta FdS_x + \Delta GdS_y\right) \tag{3.14}$$

The terms in Equation (3.14) can be grouped as follows:

$$\Delta U_i = -\frac{\Delta t}{\Delta \forall_I} \int_{cell-1} \left(F dS_x + G dS_y \right) \tag{3.15a}$$

$$\Delta U_v = \frac{\Delta t}{\Delta \forall_I} \int_{1aehg} \left(F_v dS_x + G_v dS_y \right) \tag{3.15b}$$

$$\Delta^2 U_i = -\frac{\Delta t}{2\Delta \forall_I} \int_{1ehg} \left(\Delta F dS_x + \Delta G dS_y \right) \tag{3.15c}$$

$$\Delta U_s = \frac{\Delta t}{\Delta \forall_I} \int_{cell-I} \left(S d\forall \right) \tag{3.15d}$$

Substituting above defined groups back into Equation (3.14), one can get

$$\delta U_{1I} = \frac{1}{4} \left(\Delta U_i + \Delta U_s \right) + \Delta U_v + \Delta^2 U_i \tag{3.16}$$

The inviscid term, ΔU_i in Equation (3.15a) and (3.16) can be evaluated by using trapezoidal integration rule. In this integration average fluxes are used.

$$\Delta U_i = \frac{\Delta t}{\Delta \forall_I} \left(\frac{F_1 + F_4}{2} S_{1,x} + \frac{G_1 + G_4}{2} S_{1,y} \right) - \left(\frac{F_2 + F_3}{2} S_{2,x} + \frac{G_2 + G_3}{2} S_{2,y} \right)$$

$$+ \left(\frac{F_1 + F_2}{2} S_{3,x} + \frac{G_1 + G_2}{2} S_{3,y} \right) - \left(\frac{F_3 + F_4}{2} S_{4,x} + \frac{G_3 + G_4}{2} S_{4,y} \right) \tag{3.17}$$

In the Equation (3.17), the used surface vectors used are defined according to Figure (3.2) as shown below.
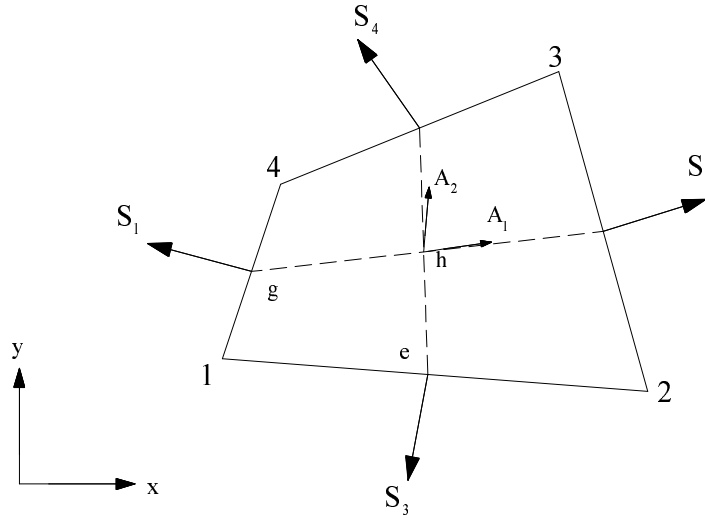
Figure 3.2 Surface vectors on cell I

Surface vectors are the projection of the faces along the axis's .For instance S_{1x} is projection of face 1 on the y axis. Therefore, the surface vectors in Equation (3.17) can be calculated easily as follows.

$$S_1 = (y_4 - y_1)\vec{i} + (x_1 - x_4)\vec{j} \qquad\qquad S_2 = (y_3 - y_2)\vec{i} + (x_2 - x_3)\vec{j} \qquad (3.18)$$

$$S_3 = (y_1 - y_2)\vec{i} + (x_1 - x_2)\vec{j} \qquad\qquad S_4 = (y_4 - y_3)\vec{i} + (x_3 - x_4)\vec{j}$$

After the evaluation of the first order inviscid changes, ΔU_i, the second order inviscid terms can be calculated using these values in each cell. As mentioned before for the integration of the second order terms, transformed control volume in cell I, which is 1ehg, is used. Calculations are performed due to the fluxes passing through the faces of e-h and g-h, which is shown in Figure 3.2. So the surface integrals are evaluated by considering these two faces. The vectors of these faces are defined as $\vec{A_1}$ and $\vec{A_2}$ as shown in Figure 3.2. Referring Figure 3.2, Equation (3.15c) can be expressed as follows:

$$\Delta^2 U_i = -\frac{\Delta t}{2\Delta \forall_I} \frac{1}{2} \{\Delta F(A_{1x} + A_{2x}) + \Delta G(A_{1y} + A_{2y})\}$$

(3.19)

where surface vectors $\vec{A}_1$ and $\vec{A}_2$ can be expressed as follows:

$$\vec{A}_1 = \frac{(y_4 + y_3) - (y_1 + y_2)}{2} \vec{i} + \frac{(x_1 + x_2) - (x_4 + x_3)}{2} \vec{j}$$

(3.20)

$$\vec{A}_2 = \frac{(y_1 + y_4) - (y_3 + y_2)}{2} \vec{i} + \frac{(x_2 + x_3) - (x_1 + x_4)}{2} \vec{j}$$

For an easier representation of Equation (3.19), following notation can be defined.

$$\Delta f_i = \Delta F \cdot A_{1x} + \Delta G \cdot A_{1y}$$

(3.21)

$$\Delta g_i = \Delta F \cdot A_{2x} + \Delta G \cdot A_{2y}$$

(3.22)

By substituting these terms into Equation (3.19) one can obtain following terms

$$\Delta^2 U_i = \frac{1}{4} \frac{\Delta t}{\Delta \forall_I} (-\Delta f_i - \Delta g_i)$$

(3.23)

So far, the first and second order inviscid flux terms have been handled. Viscous flux terms can be evaluated in the same way as the second order inviscid flux terms. The formulation of viscous flux terms given in Equation (3.15b) can be expressed as follows:

$$\Delta U_v = \frac{\Delta t}{2\Delta \forall_I} \{F_v(A_{1x} + A_{2x}) + G_v(A_{1y} + A_{2y})\}$$

(3.24)

Introducing the following notation

$$\Delta f_v = F_v \cdot A_{1x} + G_v \cdot A_{1y} \tag{3.25a}$$

$$\Delta g_v = F_v \cdot A_{2x} + G_v \cdot A_{2y} \tag{3.25b}$$

By rearranging Equation (3.24) using Equation (3.25), one can obtain

$$\Delta U_v = \frac{\Delta t}{2\Delta\forall_I}\left(\Delta f_v + \Delta g_v\right) \tag{3.26}$$

The calculation of viscous terms is completed. It should also be noted that F_v and G_v are calculated separately for each node of the cell. Calculation procedure will also be discussed in this chapter in Section 3.2.

Now, the source term, ΔU_s in Equation (3.15d) is formulated by carrying out the integral in the primary control volume as stated below.

$$\Delta U_s = \frac{\Delta t}{\Delta\forall_I} S_{center} \Delta\forall_I = \Delta t S_{center} \tag{3.27}$$

Up to now changes in node 1 due to cell-1 have been examined. The contribution of the changes in cell-I to the four nodes of this cell can be given as follows:

$$\delta U_{1I} = \frac{1}{4}\left\{\Delta U_i + \frac{\Delta t}{\Delta\forall_I}\left(\left(-\Delta f_i - \Delta g_i\right) - 2\left(-\Delta f_v - \Delta g_v\right) + \Delta\forall_I S_{center}\right)\right\} \tag{3.28a}$$

$$\delta U_{2I} = \frac{1}{4}\left\{\Delta U_i + \frac{\Delta t}{\Delta\forall_I}\left(\left(+\Delta f_i - \Delta g_i\right) - 2\left(+\Delta f_v - \Delta g_v\right) + \Delta\forall_I S_{center}\right)\right\} \tag{3.28b}$$

$$\delta U_{3I} = \frac{1}{4}\left\{\Delta U_i + \frac{\Delta t}{\Delta\forall_I}\left(\left(+\Delta f_i + \Delta g_i\right) - 2\left(+\Delta f_v + \Delta g_v\right) + \Delta\forall_I S_{center}\right)\right\} \tag{3.28c}$$

$$\delta U_{4I} = \frac{1}{4} \left\{ \Delta U_i + \frac{\Delta t}{\Delta \forall_I} \left((-\Delta f_i + \Delta g_i) - 2(-\Delta f_v + \Delta g_v) + \Delta \forall_I S_{center} \right) \right\} \tag{3.28d}$$

Finally the conservative variables can be updated at every node of the cell as follows:

$$U_1^{n+1} = U_1^n + \delta U_{1I} + \delta U_{2I} + \delta U_{3I} + \delta U_{4I} \tag{3.29}$$

3.2. CALCULATION OF VISCOUS AND HEAT CONDUCTION TERMS

The terms containing the derivative of a conservative variable is written in the physical space (x, y) can be transformed into computational space (ξ, η) for any conservative variable U.

$$(x, y) \rightarrow (\xi, \eta) \tag{3.30}$$

where

$$x = x\,(\xi, \eta) \qquad\qquad\qquad \xi = \xi(x, y) \tag{3.31}$$
$$y = y\,(\xi, \eta) \qquad\qquad\qquad \eta = \eta(x, y)$$

Using the chain rule, the transformation of derivatives can be written as:

$$\frac{\partial}{\partial x} = \xi_x \frac{\partial}{\partial \xi} + \eta_x \frac{\partial}{\partial \eta}$$

$$\tag{3.32}$$

$$\frac{\partial}{\partial y} = \xi_y \frac{\partial}{\partial \xi} + \eta_y \frac{\partial}{\partial \eta}$$

where the terms ξ_x, η_x, ξ_y and η_y are obtained with following procedure. For the transformation from *(x, y)* space to *(ξ,η)* space, the total differentials for *dx* and *dy* can be given as

$$dx = x_\xi d\xi + x_\eta d\eta$$
$$dy = y_\xi d\xi + y_\eta d\eta$$

(3.33)

or in matrix form

$$\begin{bmatrix} dx \\ dy \end{bmatrix} = \begin{bmatrix} \dfrac{\partial x}{\partial \xi} & \dfrac{\partial x}{\partial \eta} \\ \dfrac{\partial y}{\partial \xi} & \dfrac{\partial y}{\partial \eta} \end{bmatrix} \begin{bmatrix} d\xi \\ d\eta \end{bmatrix}$$

(3.34)

The jacobian of the transformation then

$$J = \begin{bmatrix} x_\xi & y_\eta \\ y_\xi & y_\eta \end{bmatrix}$$

(3.35)

For the transformation from *(ξ,η)* plane to *(x, y)* plane, the total differentials for *dη* and *dξ* are

$$d\xi = \xi_x dx + \xi_y dy$$
$$d\eta = \eta_x dx + \eta_y dy$$

(3.36)

or in matrix form

$$\begin{bmatrix} d\xi \\ d\eta \end{bmatrix} = \begin{bmatrix} \dfrac{\partial \xi}{\partial x} & \dfrac{\partial \xi}{\partial y} \\ \dfrac{\partial \eta}{\partial x} & \dfrac{\partial \eta}{\partial y} \end{bmatrix} \begin{bmatrix} dx \\ dy \end{bmatrix}$$

(3.37)

Inverse transformation is possible whenever

$$|J| = \frac{\partial x}{\partial \xi}\frac{\partial y}{\partial \eta} - \frac{\partial x}{\partial \eta}\frac{\partial y}{\partial \xi} > 0 \qquad (3.38)$$

and can be given as follows

$$\begin{bmatrix} d\xi \\ d\eta \end{bmatrix} = [J]^{-1}\begin{bmatrix} dx \\ dy \end{bmatrix} \qquad (3.39)$$

or

$$\begin{bmatrix} d\xi \\ d\eta \end{bmatrix} = \frac{1}{|J|}\begin{bmatrix} \dfrac{\partial y}{\partial \eta} & -\dfrac{\partial x}{\partial \eta} \\ -\dfrac{\partial y}{\partial \xi} & \dfrac{\partial x}{\partial \xi} \end{bmatrix}\begin{bmatrix} dx \\ dy \end{bmatrix} \qquad (3.40)$$

By equating Equations (3.37) and (3.40); one can obtain

$$\frac{1}{|J|}\begin{bmatrix} \dfrac{\partial y}{\partial \eta} & -\dfrac{\partial x}{\partial \eta} \\ -\dfrac{\partial y}{\partial \xi} & \dfrac{\partial x}{\partial \xi} \end{bmatrix}\begin{bmatrix} dx \\ dy \end{bmatrix} = \begin{bmatrix} \dfrac{\partial \xi}{\partial x} & \dfrac{\partial \xi}{\partial y} \\ \dfrac{\partial \eta}{\partial x} & \dfrac{\partial \eta}{\partial y} \end{bmatrix} \qquad (3.41)$$

Then the equations for the metric terms in the Jacobian matrix are

$$\frac{\partial \xi}{\partial x} = \frac{1}{|J|}\left(\frac{\partial y}{\partial \eta}\right) \qquad (3.42a)$$

$$\frac{\partial \xi}{\partial y} = -\frac{1}{|J|}\left(\frac{\partial x}{\partial \eta}\right) \qquad (3.42b)$$

$$\frac{\partial \eta}{\partial x} = -\frac{1}{|J|}\left(\frac{\partial y}{\partial \xi}\right) \tag{3.42c}$$

$$\frac{\partial \eta}{\partial y} = \frac{1}{|J|}\left(\frac{\partial x}{\partial \xi}\right) \tag{3.42d}$$

Now, the shear stresses can be expressed in terms of gradients in curvilinear coordinates as follows

$$\tau_{xx} = \mu\left(\frac{4}{3}\left(\frac{\partial \xi}{\partial x}\frac{\partial u}{\partial \xi} + \frac{\partial \eta}{\partial x}\frac{\partial u}{\partial \eta}\right) - \frac{2}{3}\left(\frac{\partial \xi}{\partial y}\frac{\partial v}{\partial \xi} + \frac{\partial \eta}{\partial y}\frac{\partial v}{\partial \eta}\right)\right) \tag{3.43a}$$

$$\tau_{yy} = \mu\left(\frac{4}{3}\left(\frac{\partial \xi}{\partial y}\frac{\partial v}{\partial \xi} + \frac{\partial \eta}{\partial y}\frac{\partial v}{\partial \eta}\right) - \frac{2}{3}\left(\frac{\partial \xi}{\partial x}\frac{\partial u}{\partial \xi} + \frac{\partial \eta}{\partial x}\frac{\partial u}{\partial \eta}\right)\right) \tag{3.43b}$$

$$\tau_{xy} = \mu\left(\left(\frac{\partial \xi}{\partial y}\frac{\partial v}{\partial \xi} + \frac{\partial \eta}{\partial y}\frac{\partial v}{\partial \eta}\right) + \left(\frac{\partial \xi}{\partial x}\frac{\partial u}{\partial \xi} + \frac{\partial \eta}{\partial x}\frac{\partial u}{\partial \eta}\right)\right) \tag{3.43c}$$

and the heat flux equations can be expressed as

$$q_x = -\left(\frac{\mu}{\Pr}\right)\frac{1}{(\gamma-1)}\left(\frac{\partial \xi}{\partial x}\frac{\partial T}{\partial \xi} + \frac{\partial \eta}{\partial x}\frac{\partial T}{\partial \eta}\right) \tag{3.44a}$$

$$q_y = -\left(\frac{\mu}{\Pr}\right)\frac{1}{(\gamma-1)}\left(\frac{\partial \xi}{\partial y}\frac{\partial T}{\partial \xi} + \frac{\partial \eta}{\partial y}\frac{\partial T}{\partial \eta}\right) \tag{3.44b}$$

Ni [14] suggested that, first order finite difference approximation to the above derivatives can be formulated in each cell separately for each node as follows:

Let Q denote any conservative variable or a Cartesian coordinate x or y, then for node 1 of cell I, one can write the following expressions for $\left(\dfrac{\partial Q}{\partial \xi}\right)_1$ and $\left(\dfrac{\partial Q}{\partial \eta}\right)_1$ as follows:

$$\left(\frac{\partial Q}{\partial \xi}\right)_1 \cong \frac{\Delta Q}{\Delta \xi} = \frac{Q_2 - Q_1}{\xi_2 - \xi_1} = \frac{Q_2 - Q_1}{\Delta \xi} = Q_2 - Q_1 \tag{3.45a}$$

$$\left(\frac{\partial Q}{\partial \eta}\right)_1 \cong \frac{\Delta Q}{\Delta \eta} = \frac{Q_4 - Q_1}{\eta_4 - \eta_1} = \frac{Q_4 - Q_1}{\Delta \eta} = Q_4 - Q_1 \tag{3.45b}$$

The derivatives for the other nodes can be handled in a similar way: The idea is to remain in the cell, and use either a forward or a backward difference, whichever appropriate.

3.3. ARTIFICIAL SMOOTHING

The second-order Lax-Wendroff scheme gives satisfactory results in the regions where the variation of the properties is smooth. The major drawback of the scheme is that it causes oscillations around the discontinuities; around a shock wave or in the boundary layer etc. So in order to damp these oscillations, artificial smoothing terms must be introduced.

So in this study, artificial smoothing terms are added to the distribution formulas, given by Equations 3.28.a-h. The artificial smoothing terms consist of second-order and fourth order damping terms. The second order smoothing terms method is supplied from Ni [].On the other hand the fourth-order damping terms are taken from Tınaztepe [15]. These terms can be given as follows:

$$\delta^2 U_i = \sigma^2 \frac{\Delta t}{4 \Delta V} \Delta A \left(\overline{U} - U_i\right) \tag{3.46a}$$

$$\delta^4 U_i = \sigma^4 \frac{\Delta t}{4 \Delta V} \Delta A \left(\overline{\delta^2 U} - \delta^2 U_i \right) \qquad (3.46b)$$

In the above equations, the subscript i denotes the node number of a cell and the barred quantities denotes the conservative variables averaged over the cell. ΔA is related to areas of the cell at the cell center, as shown in Figure 3.2 and given as follows:

$$\Delta A = \sqrt{\left| \vec{A}_1 \right|^2 + \left| \vec{A}_2 \right|^2} \qquad (3.47)$$

Also σ^2 and σ^4 terms in Equations (3.45a) and (3.45b) are the second and fourth order artificial smoothing coefficients, respectively. σ^4 should be taken as 1/32 of σ^2 as specified by Tınaztepe[17].

Ni [14] states that near the solid walls artificial smoothing term should be decreased as much as possible due to the fact that the viscous fluxes in the momentum equations are quite large and adequate to provide smoothing near the solid boundaries [14,18]. Considering this fact Mach number scaling is used. The second order artificial smoothing coefficient is reduced by the local Mach number scaling and it is given by Tınaztepe[17].

$$\left(\sigma^2 \right)_{scaled} = \left(\frac{M}{M_\infty} \right)^2 \sigma^2 \qquad (3.48)$$

Finally, the total change of a node can be written as follows

$$\delta U_i = \delta U_i + \delta^2 U_i + \delta^4 U_i \qquad i = 1,..,4 \qquad (3.49)$$

3.4. TIME STEPPING CONTROL

The Lax-Wendroff scheme is an explicit scheme, which marches in time; In all explicit methods, a limit must be prescribed for the time step at every iteration, otherwise the stability of the method will be endangered.   This limit is superimposed on the time step Δt by the CFL condition [14].

In this study, Ni's [14] formulation is used to restrict the time step for the solution of the Navier-Stokes equations and can be given as

$$
\Delta t = CFL \cdot \min \left[\frac{\left| \vec{L}_x \right|}{\left| V \cdot \vec{l} \right| + c + \dfrac{2\mu}{\left| \vec{L}_x \right|}} , \quad \frac{\left| \vec{L}_y \right|}{\left| V \cdot \vec{l} \right| + c + \dfrac{2\mu}{\left| \vec{L}_y \right|}} \right]
$$

(3.50)

where $\vec{L}$ is the displacement vector crossing the cell in the streamwise direction, $\vec{l}$ is a unit vector in the direction $\vec{L}$, c is the local speed of sound in the cell and μ is the viscosity.

$\vec{L}$ can be expressed in the x and y directions, as

$$
\vec{L}_x = \left\{ \left[\frac{1}{2}(x_2 + x_3) - \frac{1}{2}(x_1 + x_4) \right] \vec{i} + \left[\frac{1}{2}(y_2 + y_3) - \frac{1}{2}(y_1 + y_4) \right] \vec{j} \right\}
$$
(3.51a)

and

$$
\vec{L}_y = \left\{ \left[\frac{1}{2}(x_3 + x_4) - \frac{1}{2}(x_1 + x_2) \right] \vec{i} + \left[\frac{1}{2}(y_3 + y_4) - \frac{1}{2}(y_1 + y_2) \right] \vec{j} \right\}
$$
(3.51b)

respectively.

For stability of the scheme, CFL number stays below 1.0 for every cell in the computational domain. Local time stepping control is employed, that is a different Δt value is imposed on each cell. All of the variables used in this method are taken as average values over a cell.

3.5. DISCRETIZATION OF THE SPALART-ALLMARAS TURBULENCE EQUATION BY FINITE DIFFERENCE METHOD

Spalart-Allmaras model is also solved uncoupled to Navier Stokes equations in this study. Finite difference method, which is explicit in time, is used to discretized the Spalart-Allmaras turbulence equation [12]. Discretization procedure in finite difference method is given in Hoffmann [11]. The derivatives in Spalart-Almaras equation given by Cartesian derivatives given in Equation (2.16) can be written in the computational space as follows [11].

$$\frac{\partial \overline{v}}{\partial t} + U \frac{\partial \overline{v}}{\partial \xi} + V \frac{\partial \overline{v}}{\partial \eta} = \frac{(1+C_{b2})}{\sigma} \left\{ \xi_x \frac{\partial \alpha}{\partial \xi} + \eta_x \frac{\partial \alpha}{\partial \eta} + \xi_y \frac{\partial \beta}{\partial \xi} + \eta_y \frac{\partial \beta}{\partial \eta} \right\}$$

$$- \frac{C_{b2}}{\sigma} (v + \overline{v}) \left\{ \xi_x \frac{\partial A}{\partial \xi} + \eta_x \frac{\partial A}{\partial \eta} + \xi_y \frac{\partial B}{\partial \xi} + \eta_y \frac{\partial B}{\partial \eta} \right\} + \frac{C_{b1}}{\kappa^2} \left[(1-f_{t2})f_{v2} + f_{t2} \left(\frac{\overline{v}}{d} \right)^2 \right]$$

$$- (C_{w1}f_w) \left(\frac{\overline{v}}{d} \right)^2 + C_{b1}(1-f_{t2})S\overline{v} + f_{t1}(\Delta q)^2$$

(3.52)

where

$$A = \frac{\partial \overline{v}}{\partial x} = \xi_x \frac{\partial \overline{v}}{\partial \xi} + \eta_x \frac{\partial \overline{v}}{\partial \eta}$$

(3.53)

$$B = \frac{\partial \overline{v}}{\partial y} = \xi_y \frac{\partial \overline{v}}{\partial \xi} + \eta_y \frac{\partial \overline{v}}{\partial \eta}$$

$$\alpha = (v + \bar{v})\, (\xi_x \frac{\partial \bar{v}}{\partial \xi} + \eta_x \frac{\partial \bar{v}}{\partial \eta}) \tag{3.54}$$

$$\beta = (v + \bar{v})\, (\xi_y \frac{\partial \bar{v}}{\partial \xi} + \eta_y \frac{\partial \bar{v}}{\partial \eta})$$

$$S = \left| \xi_y \frac{\partial u}{\partial \xi} + \eta_y \frac{\partial u}{\partial \eta} - (\xi_x \frac{\partial v}{\partial \xi} + \eta_x \frac{\partial v}{\partial \eta}) \right| \tag{3.55}$$

A first order upwind method is used for the convective terms First order upwind approximation yields [11]

$$-(U \frac{\partial \bar{v}}{\partial \xi} + V \frac{\partial \bar{v}}{\partial \eta}) = -\left\{ \frac{1}{2}(U_{i,j} + |U_{i,j}|)(\frac{\bar{v}_{i,j} - \bar{v}_{i-1,j}}{\Delta \xi}) + \frac{1}{2}(U_{i,j} - |U_{i,j}|)(\frac{\bar{v}_{i+1,j} - \bar{v}_{i-1,j}}{\Delta \xi}) \right.$$

$$\left. + \frac{1}{2}(V_{i,j} + |V_{i,j}|)(\frac{\bar{v}_{i,j} - \bar{v}_{i,j-1}}{\Delta \eta}) + \frac{1}{2}(V_{i,j} - |V_{i,j}|)(\frac{\bar{v}_{i,j+1} - \bar{v}_{i,j}}{\Delta \eta}) \right\}$$

$$\tag{3.56}$$

For the diffusion terms a second order central difference approximation is used. Discretization of the two derivative terms are shown below, discretization of the other diffusion terms are similar. For more details one can refer to Hoffman [11].

$$\xi_x \frac{\partial \alpha}{\partial \xi} + \xi_y \frac{\partial \beta}{\partial \xi} = \xi_{x\,i,j} \frac{\alpha_{i+\frac{1}{2},j} - \alpha_{i-\frac{1}{2},j}}{\Delta \xi} + \xi_{y\,i,j} \frac{\beta_{i+\frac{1}{2},j} - \beta_{i-\frac{1}{2},j}}{\Delta \xi} \tag{3.57}$$

where

$$\alpha_{i+\frac{1}{2},j} = (v + \bar{v})_{i+\frac{1}{2},j} \left[\xi_{x_{i+\frac{1}{2},j}} \left(\frac{\bar{v}_{i+1,j} - \bar{v}_{i,j}}{\Delta \xi} \right) + \eta_{x_{i+\frac{1}{2},j}} \left(\frac{\bar{v}_{i+\frac{1}{2},j+\frac{1}{2}} - \bar{v}_{i+\frac{1}{2},j-\frac{1}{2}}}{\Delta \eta} \right) \right] \tag{3.58a}$$

$$\alpha_{i-\frac{1}{2},j} = (v+\overline{v})_{i-\frac{1}{2},j}\left[\xi_{x_{i-\frac{1}{2},j}}\left(\frac{\overline{v}_{i,j}-\overline{v}_{i-1,j}}{\Delta\xi}\right)+\eta_{x_{i-\frac{1}{2},j}}\left(\frac{\overline{v}_{i-\frac{1}{2},j+\frac{1}{2}}-\overline{v}_{i-\frac{1}{2},j-\frac{1}{2}}}{\Delta\eta}\right)\right]$$

$$\beta_{i+\frac{1}{2},j} = (v+\overline{v})_{i+\frac{1}{2},j}\left[\xi_{y_{i+\frac{1}{2},j}}\left(\frac{\overline{v}_{i+1,j}-\overline{v}_{i,j}}{\Delta\xi}\right)+\eta_{y_{i+\frac{1}{2},j}}\left(\frac{\overline{v}_{i+\frac{1}{2},j+\frac{1}{2}}-\overline{v}_{i+\frac{1}{2},j-\frac{1}{2}}}{\Delta\eta}\right)\right]$$

$$\tag{3.58b}$$

$$\beta_{i-\frac{1}{2},j} = (v+\overline{v})_{i-\frac{1}{2},j}\left[\xi_{y_{i-\frac{1}{2},j}}\left(\frac{\overline{v}_{i+1,j}-\overline{v}_{i,j}}{\Delta\xi}\right)+\eta_{y_{i-\frac{1}{2},j}}\left(\frac{\overline{v}_{i+\frac{1}{2},j+\frac{1}{2}}-\overline{v}_{i+\frac{1}{2},j-\frac{1}{2}}}{\Delta\eta}\right)\right]$$

Complete explicit formulation, which is also given in Hoffmann [11] is stated as follows:

$$\overline{v}^{n+1}_{i,j} = \overline{v}^{n}_{i,j} - \Delta t\left\{\frac{1}{2}\left(U_{i,j}+|U_{i,j}|\right)\left(\frac{\overline{v}_{i,j}-\overline{v}_{i-1,j}}{\Delta\xi}\right)+\frac{1}{2}\left(U_{i,j}-|U_{i,j}|\right)\left(\frac{\overline{v}_{i+1,j}-\overline{v}_{i,j}}{\Delta\xi}\right)\right.$$

$$\left.+\frac{1}{2}\left(V_{i,j}+|V_{i,j}|\right)\left(\frac{\overline{v}_{i,j}-\overline{v}_{i,j-1}}{\Delta\eta}\right)+\frac{1}{2}\left(V_{i,j}-|V_{i,j}|\right)\left(\frac{\overline{v}_{i,j+1}-\overline{v}_{i,j}}{\Delta\eta}\right)\right\}$$

$$+\Delta t\left(\frac{1+C_{b2}}{\sigma}\right)\left[(v+\overline{v})_{i+\frac{1}{2},j}\left\{(\xi_{x_{i,j}}\xi_{x_{i+\frac{1}{2},j}}+\xi_{y_{i,j}}\xi_{y_{i+\frac{1}{2},j}})\left[\frac{\overline{v}_{i+1,j}-\overline{v}_{i,j}}{(\Delta\xi)^2}\right]\right\}\right.$$

$$-(v+\overline{v})_{i-\frac{1}{2},j}\left\{(\xi_{x_{i,j}}\xi_{x_{i-\frac{1}{2},j}}+\xi_{y_{i,j}}\xi_{y_{i-\frac{1}{2},j}})\left[\frac{\overline{v}_{i,j}-\overline{v}_{i-1,j}}{(\Delta\xi)^2}\right]\right\}$$

$$+(v+\overline{v})_{i+\frac{1}{2},j}\left\{(\xi_{x_{i,j}}\eta_{x_{i+\frac{1}{2},j}}+\xi_{y_{i,j}}\eta_{y_{i+\frac{1}{2},j}})\left[\frac{\overline{v}_{i+\frac{1}{2},j+\frac{1}{2}}-\overline{v}_{i+\frac{1}{2},j-\frac{1}{2}}}{\Delta\xi\Delta\eta}\right]\right\}$$

$$- (\nu + \overline{\nu})_{i-\frac{1}{2},j} \left\{ (\xi_{x_{i,j}} \eta_{x_{i+\frac{1}{2},j}} + \xi_{y_{i,j}} \eta_{y_{i-\frac{1}{2},j}}) \left[\frac{\overline{\nu}_{i-\frac{1}{2},j+\frac{1}{2}} - \overline{\nu}_{i-\frac{1}{2},j-\frac{1}{2}}}{\Delta\xi\Delta\eta} \right] \right\}$$

$$+ (\nu + \overline{\nu})_{i,j+\frac{1}{2}} \left\{ (\eta_{x_{i,j}} \eta_{x_{i+\frac{1}{2},j}} + \eta_{y_{i,j}} \eta_{y_{i,j+\frac{1}{2}}}) \left[\frac{\overline{\nu}_{i,j+1} - \overline{\nu}_{i,j}}{(\Delta\eta)^2} \right] \right\}$$

$$- (\nu + \overline{\nu})_{i,j+\frac{1}{2}} \left\{ (\eta_{x_{i,j}} \eta_{x_{i,j-\frac{1}{2}}} + \eta_{y_{i,j}} \eta_{y_{i,j-\frac{1}{2}}}) \left[\frac{\overline{\nu}_{i,j} - \overline{\nu}_{i,j-1}}{(\Delta\eta)^2} \right] \right\}$$

$$+ (\nu + \overline{\nu})_{i,j+\frac{1}{2}} \left\{ (\eta_{x_{i,j}} \xi_{x_{i,j+\frac{1}{2}}} + \eta_{y_{i,j}} \xi_{y_{i,j+\frac{1}{2}}}) \left[\frac{\overline{\nu}_{i+\frac{1}{2},j+\frac{1}{2}} - \overline{\nu}_{i-\frac{1}{2},j+\frac{1}{2}}}{\Delta\xi\Delta\eta} \right] \right\}$$

$$- (\nu + \overline{\nu})_{i,j-\frac{1}{2}} \left\{ (\eta_{x_{i,j}} \xi_{x_{i,j-\frac{1}{2}}} + \eta_{y_{i,j}} \xi_{y_{i,j-\frac{1}{2}}}) \left[\frac{\overline{\nu}_{i+\frac{1}{2},j-\frac{1}{2}} - \overline{\nu}_{i-\frac{1}{2},j-\frac{1}{2}}}{\Delta\xi\Delta\eta} \right] \right\}$$

$$+ \Delta t \left(\frac{C_{b2}}{\sigma} \right) \left[- (\nu + \overline{\nu})_{i,j} \left\{ (\xi_{x_{i,j}} \xi_{x_{i+\frac{1}{2},j}} + \xi_{y_{i,j}} \xi_{y_{i+\frac{1}{2},j}}) \left[\frac{\overline{\nu}_{i+1,j} - \overline{\nu}_{i,j}}{(\Delta\xi)^2} \right] \right\} \right.$$

$$+ (\nu + \overline{\nu})_{i,j} \left\{ (\xi_{x_{i,j}} \xi_{x_{i-\frac{1}{2},j}} + \xi_{y_{i,j}} \xi_{y_{i-\frac{1}{2},j}}) \left[\frac{\overline{\nu}_{i,j} - \overline{\nu}_{i-1,j}}{(\Delta\xi)^2} \right] \right\}$$

$$- (\nu + \overline{\nu})_{i,j} \left\{ (\xi_{x_{i,j}} \eta_{x_{i+\frac{1}{2},j}} + \xi_{y_{i,j}} \eta_{y_{i+\frac{1}{2},j}}) \left[\frac{\overline{\nu}_{i+\frac{1}{2},j+\frac{1}{2}} - \overline{\nu}_{i+\frac{1}{2},j-\frac{1}{2}}}{\Delta\eta\Delta\xi} \right] \right\}$$

$$+ (\nu + \overline{\nu})_{i,j} \left\{ (\xi_{x_{i,j}} \eta_{x_{i-\frac{1}{2},j}} + \xi_{y_{i,j}} \eta_{y_{i-\frac{1}{2},j}}) \left[\frac{\overline{\nu}_{i-\frac{1}{2},j+\frac{1}{2}} - \overline{\nu}_{i-\frac{1}{2},j-\frac{1}{2}}}{\Delta\eta\,\Delta\xi} \right] \right\}$$

$$- (\nu + \overline{\nu})_{i,j} \left\{ (\eta_{x_{i,j}} \eta_{x_{i,j+\frac{1}{2}}} + \eta_{y_{i,j}} \eta_{y_{i,j+\frac{1}{2}}}) \left[\frac{\overline{\nu}_{i,j+1} - \overline{\nu}_{i,j}}{(\Delta\eta)^2} \right] \right\}$$

$$+ (\nu + \bar{\nu})_{i,j} \left\{ \left(\eta_{x_{i,j}} \eta_{x_{i,j+\frac{1}{2}}} + \eta_{y_{i,j}} \eta_{y_{i,j+\frac{1}{2}}} \right) \left[\frac{\bar{\nu}_{i,j} - \bar{\nu}_{i,j,j-1}}{(\Delta\eta)^2} \right] \right\}$$

$$- (\nu + \bar{\nu})_{i,j} \left\{ \left(\eta_{x_{i,j}} \xi_{x_{i,j+\frac{1}{2}}} + \eta_{y_{i,j}} \eta_{y_{i,j+\frac{1}{2}}} \right) \left[\frac{\bar{\nu}_{i+\frac{1}{2},j+\frac{1}{2}} - \bar{\nu}_{i-\frac{1}{2},j+\frac{1}{2}}}{\Delta\eta\,\Delta\xi} \right] \right\}$$

$$+ (\nu + \bar{\nu})_{i,j} \left\{ \left(\eta_{x_{i,j}} \xi_{x_{i,j+\frac{1}{2}}} + \eta_{y_{i,j}} \xi_{y_{i,j-\frac{1}{2}}} \right) \left[\frac{\bar{\nu}_{i+\frac{1}{2},j-\frac{1}{2}} - \bar{\nu}_{i-\frac{1}{2},j-\frac{1}{2}}}{\Delta\eta\,\Delta\xi} \right] \right\}$$

$$+ \Delta t \left\{ C_{b1} \bar{S} \bar{\nu}_{i,j} (1 - f_{t2}) - \left(c_{w1} f_w - \frac{c_{b1}}{\kappa^2} f_{t2} \right) \left(\frac{\bar{\nu}_{i,j}}{d} \right)^2 + f_{t1} (\Delta q)^2 \right\}$$

$$(3.59)$$

3.6. DISCRETIZATION OF THE BALDWIN-BARTH TURBULENCE EQUATION BY FINITE DIFFERENCE METHOD

Since equations of both Spalart-Allmaras and Baldwin-Barth turbulence equation are similar, same explicit finite difference discretization procedure, as applied to Spalart-Allmaras, is also applied to Baldwin-Barth turbulence Equation [2.26]. Equation (2.26) can be stated in computational space as follows:

$$\frac{\partial R}{\partial t} + U \frac{\partial R}{\partial \xi} + V \frac{\partial R}{\partial \eta} = -\frac{1}{\sigma_\varepsilon} \left\{ \xi_x \frac{\partial \alpha}{\partial \xi} + \eta_x \frac{\partial \alpha}{\partial \eta} + \xi_y \frac{\partial \beta}{\partial \xi} + \eta_y \frac{\partial \beta}{\partial \eta} \right\}$$

$$+ 2 * \left(\nu + \frac{\nu_t}{\sigma_\varepsilon} \right) \left\{ \xi_x \frac{\partial A}{\partial \xi} + \eta_x \frac{\partial A}{\partial \eta} + \xi_y \frac{\partial B}{\partial \xi} + \eta_y \frac{\partial B}{\partial \eta} \right\}$$

$$+ (C_{\varepsilon 2} f_2 - C_{\varepsilon 1}) \sqrt{C_\mu D_1 D_2} \, SR \qquad (3.60)$$

where

$$R = v\,\overline{\mathrm{Re}}_T \qquad\qquad [3.61]$$

$$A = \frac{\partial R}{\partial x} = \xi_x \frac{\partial R}{\partial \xi} + \eta_x \frac{\partial R}{\partial \eta}$$

$$\qquad\qquad (3.62)$$

$$B = \frac{\partial R}{\partial y} = \xi_y \frac{\partial R}{\partial \xi} + \eta_y \frac{\partial R}{\partial \eta}$$

$$\alpha = v_t\,(\xi_x \frac{\partial \overline{v}}{\partial \xi} + \eta_x \frac{\partial \overline{v}}{\partial \eta})$$

$$\qquad\qquad (3.63)$$

$$\beta = v_t\,(\xi_y \frac{\partial \overline{v}}{\partial \xi} + \eta_y \frac{\partial \overline{v}}{\partial \eta})$$

$$S^2 = a_1\left(\frac{\partial u}{\partial \xi}\right)^2 + b_1\left(\frac{\partial u}{\partial \eta}\right)^2 + a_2\left(\frac{\partial v}{\partial \xi}\right)^2 + b_2\left(\frac{\partial v}{\partial \eta}\right)^2 + 2c_1\left(\frac{\partial u}{\partial \xi}\,\frac{\partial u}{\partial \eta}\right)$$

$$+ 2c_2\left(\frac{\partial v}{\partial \xi}\,\frac{\partial v}{\partial \eta}\right) + 2a_3\left(\frac{\partial u}{\partial \xi}\,\frac{\partial v}{\partial \eta}\right) + 2b_3\left(\frac{\partial u}{\partial \eta}\,\frac{\partial v}{\partial \eta}\right) + 2c_3\left(\frac{\partial u}{\partial \xi}\,\frac{\partial v}{\partial \eta}\right)$$

$$+ 2c_4\left(\frac{\partial u}{\partial \eta}\,\frac{\partial v}{\partial \xi}\right) \qquad\qquad (3.64)$$

where the coefficients of $a_1, a_2, a_3, b_1, b_2, b_3, c_1, c_2, c_3$ and c_4 given in above equation are defined in Appendix.

A first order upwind method is used for the convective terms. First order upwind approximation yields [11]

$$-(U\frac{\partial R}{\partial \xi}+V\frac{\partial R}{\partial \eta})=-\left\{\frac{1}{2}(U_{i,j}+\left|U_{i,j}\right|)(\frac{R_{i,j}-R_{i-1,j}}{\Delta \xi})+\frac{1}{2}(U_{i,j}-\left|U_{i,j}\right|)(\frac{R_{i+1,j}-R_{i-1,j}}{\Delta \xi})\right.$$

$$\left.+\frac{1}{2}(V_{i,j}+\left|V_{i,j}\right|)(\frac{R_{i,j}-R_{i,j-1}}{\Delta \eta})+\frac{1}{2}(V_{i,j}-\left|V_{i,j}\right|)(\frac{R_{i,j+1}-R_{i,j}}{\Delta \eta})\right\}$$

(3.65)

For the diffusion terms a second order central difference approximation is used [11]. Discretization of the two derivative terms are shown below, discretization of the other diffusion terms are similar. For more details one can refer to Hoffman [11].

$$\xi_x\frac{\partial \alpha}{\partial \xi}+\xi_y\frac{\partial \beta}{\partial \xi}=\xi_{xi,j}\frac{\alpha_{i+\frac{1}{2},j}-\alpha_{i-\frac{1}{2},j}}{\Delta \xi}+\xi_{yi,j}\frac{\beta_{i+\frac{1}{2},j}-\beta_{i-\frac{1}{2},j}}{\Delta \xi}$$

(3.66)

where

$$\alpha_{i+\frac{1}{2},j}=\nu_{t_{i+\frac{1}{2},j}}\left[\xi_{x_{i+\frac{1}{2},j}}\left(\frac{R_{i+1,j}-R_{i,j}}{\Delta \xi}\right)+\eta_{x_{i+\frac{1}{2},j}}\left(\frac{R_{i+\frac{1}{2},j+\frac{1}{2}}-R_{i+\frac{1}{2},j-\frac{1}{2}}}{\Delta \eta}\right)\right]$$

(3.67a)

$$\alpha_{i-\frac{1}{2},j}=\nu_{t_{i-\frac{1}{2},j}}\left[\xi_{x_{i-\frac{1}{2},j}}\left(\frac{R_{i,j}-R_{i-1,j}}{\Delta \xi}\right)+\eta_{x_{i-\frac{1}{2},j}}\left(\frac{R_{i-\frac{1}{2},j+\frac{1}{2}}-R_{i-\frac{1}{2},j-\frac{1}{2}}}{\Delta \eta}\right)\right]$$

$$\beta_{i+\frac{1}{2},j}=\nu_{t_{i+\frac{1}{2},j}}\left[\xi_{y_{i+\frac{1}{2},j}}\left(\frac{R_{i+1,j}-R_{i,j}}{\Delta \xi}\right)+\eta_{y_{i+\frac{1}{2},j}}\left(\frac{R_{i+\frac{1}{2},j+\frac{1}{2}}-R_{i+\frac{1}{2},j-\frac{1}{2}}}{\Delta \eta}\right)\right]$$

(3.67b)

$$\beta_{i-\frac{1}{2},j}=\nu_{t_{i-\frac{1}{2},j}}\left[\xi_{y_{i-\frac{1}{2},j}}\left(\frac{R_{i+1,j}-R_{i,j}}{\Delta \xi}\right)+\eta_{y_{i-\frac{1}{2},j}}\left(\frac{R_{i+\frac{1}{2},j+\frac{1}{2}}-R_{i+\frac{1}{2},j-\frac{1}{2}}}{\Delta \eta}\right)\right]$$

Complete explicit formulation which is also given in Hoffmann [19] is stated as follows

$$R^{n+1}{}_{i,j} = R^{n}{}_{i,j} - \Delta t \left\{ \frac{1}{2} \left(U_{i,j} + |U_{i,j}|\right) \left(\frac{R_{i,j} - R_{i-1,j}}{\Delta \xi}\right) + \frac{1}{2}\left(U_{i,j} - |U_{i,j}|\right)\left(\frac{R_{i+1,j} - R_{i,j}}{\Delta \xi}\right) \right.$$

$$\left. + \frac{1}{2}\left(V_{i,j} + |V_{i,j}|\right)\left(\frac{\overline{V}_{i,j} - \overline{V}_{i,j-1}}{\Delta \eta}\right) + \frac{1}{2}\left(V_{i,j} - |V_{i,j}|\right)\left(\frac{\overline{V}_{i,j+1} - \overline{V}_{i,j}}{\Delta \eta}\right) \right\}$$

$$- \Delta t \left(\frac{1}{\sigma_\varepsilon}\right) \left[\nu_{i+\frac{1}{2},j} \left\{ \left(\xi_{x_{i,j}}\xi_{x_{i+\frac{1}{2},j}} + \xi_{y_{i,j}}\xi_{y_{i+\frac{1}{2},j}}\right)\left[\frac{R_{i+1,j} - R_{i,j}}{(\Delta \xi)^2}\right] \right\} \right.$$

$$- \nu_{i-\frac{1}{2},j} \left\{ \left(\xi_{x_{i,j}}\xi_{x_{i-\frac{1}{2},j}} + \xi_{y_{i,j}}\xi_{y_{i-\frac{1}{2},j}}\right)\left[\frac{R_{i,j} - R_{i-1,j}}{(\Delta \xi)^2}\right] \right\}$$

$$+ \nu_{i+\frac{1}{2},j} \left\{ \left(\xi_{x_{i,j}}\eta_{x_{i+\frac{1}{2},j}} + \xi_{y_{i,j}}\eta_{y_{i+\frac{1}{2},j}}\right)\left[\frac{R_{i+\frac{1}{2},j+\frac{1}{2}} - R_{i+\frac{1}{2},j-\frac{1}{2}}}{\Delta \xi \Delta \eta}\right] \right\}$$

$$- \nu_{i-\frac{1}{2},j} \left\{ \left(\xi_{x_{i,j}}\eta_{x_{i-\frac{1}{2},j}} + \xi_{y_{i,j}}\eta_{y_{i-\frac{1}{2},j}}\right)\left[\frac{R_{i-\frac{1}{2},j+\frac{1}{2}} - R_{i-\frac{1}{2},j-\frac{1}{2}}}{\Delta \xi \Delta \eta}\right] \right\}$$

$$+ \nu_{i,j+\frac{1}{2}} \left\{ \left(\eta_{x_{i,j}}\eta_{x_{i+\frac{1}{2},j}} + \eta_{y_{i,j}}\eta_{y_{i,j+\frac{1}{2}}}\right)\left[\frac{R_{i,j+1} - R_{i,j}}{(\Delta \eta)^2}\right] \right\}$$

$$- \nu_{i,j-\frac{1}{2}} \left\{ \left(\eta_{x_{i,j}}\eta_{x_{i,j-\frac{1}{2}}} + \eta_{y_{i,j}}\eta_{y_{i,j-\frac{1}{2}}}\right)\left[\frac{R_{i,j} - R_{i,j-1}}{(\Delta \eta)^2}\right] \right\}$$

$$+\nu_{i,j+\frac{1}{2}}\left\{(\eta_{x_{i,j}}\xi_{x_{i,j+\frac{1}{2}}}+\eta_{y_{i,j}}\xi_{y_{i,j+\frac{1}{2}}})\left[\frac{R_{i+\frac{1}{2},j+\frac{1}{2}}-R_{i-\frac{1}{2},j+\frac{1}{2}}}{\Delta\xi\Delta\eta}\right]\right\}$$

$$-\nu_{i,j-\frac{1}{2}}\left\{(\eta_{x_{i,j}}\xi_{x_{i,j-\frac{1}{2}}}+\eta_{y_{i,j}}\xi_{y_{i,j-\frac{1}{2}}})\left[\frac{R_{i+\frac{1}{2},j-\frac{1}{2}}-R_{i-\frac{1}{2},j-\frac{1}{2}}}{\Delta\xi\Delta\eta}\right]\right\}$$

$$+\Delta t\left(\frac{2}{\sigma_\varepsilon}\right)\left[\left(\nu+\frac{\nu_t}{\sigma_\varepsilon}\right)_{i,j}\left\{(\xi_{x_{i,j}}\xi_{x_{i+\frac{1}{2},j}}+\xi_{y_{i,j}}\xi_{y_{i+\frac{1}{2},j}})\left[\frac{R_{i+1,j}-R_{i,j}}{(\Delta\xi)^2}\right]\right.\right.$$

$$-\left\{(\xi_{x_{i,j}}\xi_{x_{i-\frac{1}{2},j}}+\xi_{y_{i,j}}\xi_{y_{i-\frac{1}{2},j}})\left[\frac{R_{i,j}-R_{i-1,j}}{(\Delta\xi)^2}\right]\right\}$$

$$+\left\{(\xi_{x_{i,j}}\eta_{x_{i+\frac{1}{2},j}}+\xi_{y_{i,j}}\eta_{y_{i+\frac{1}{2},j}})\left[\frac{R_{i+\frac{1}{2},j+\frac{1}{2}}-R_{i+\frac{1}{2},j-\frac{1}{2}}}{\Delta\eta\Delta\xi}\right]\right\}$$

$$-\left\{(\xi_{x_{i,j}}\eta_{x_{i-\frac{1}{2},j}}+\xi_{y_{i,j}}\eta_{y_{i-\frac{1}{2},j}})\left[\frac{R_{i-\frac{1}{2},j+\frac{1}{2}}-R_{i-\frac{1}{2},j-\frac{1}{2}}}{\Delta\eta\,\Delta\xi}\right]\right\}$$

$$+\left\{(\eta_{x_{i,j}}\eta_{x_{i,j+\frac{1}{2}}}+\eta_{y_{i,j}}\eta_{y_{i,j+\frac{1}{2}}})\left[\frac{R_{i,j+1}-R_{i,j}}{(\Delta\eta)^2}\right]\right\}$$

$$-\left\{(\eta_{x_{i,j}}\eta_{x_{i,j+\frac{1}{2}}}+\eta_{y_{i,j}}\eta_{y_{i,j+\frac{1}{2}}})\left[\frac{R_{i,j}-R_{i,j-1}}{(\Delta\eta)^2}\right]\right\}$$

$$+\left\{(\eta_{x_{i,j}}\xi_{x_{i,j+\frac{1}{2}}}+\eta_{y_{i,j}}\eta_{y_{i,j+\frac{1}{2}}})\left[\frac{R_{i+\frac{1}{2},j+\frac{1}{2}}-R_{i-\frac{1}{2},j+\frac{1}{2}}}{\Delta\eta\,\Delta\xi}\right]\right\}$$

$$- \left\{ \left(\eta_{x_{i,j}} \xi_{x_{i,j+\frac{1}{2}}} + \eta_{y_{i,j}} \xi_{y_{i,j+\frac{1}{2}}} \right) \left[\frac{R_{i+\frac{1}{2},j-\frac{1}{2}} - R_{i-\frac{1}{2},j-\frac{1}{2}}}{\Delta \eta \, \Delta \xi} \right] \right\} \right]$$

$$+ \Delta t \left\{ (c_{\varepsilon 2} f_2 - c_{\varepsilon 1}) \sqrt{c_\mu D_1 D_2} \, SR \right\}$$

$$(3.68)$$

CHAPTER 4

INITIAL AND BOUNDARY CONDITIONS

In this chapter, the initial and boundary conditions, which are necessary to obtain a solution of the governing equations, are discussed.

In order to start up time marching computations initial conditions should be specified. The initial conditions give the state of fluid at time t=0 or at the first step of the iterative scheme. It is obvious that if the initial guess is made better, the solution will be obtained better and the probability of breakdown of the numerical process will be reduced [1]. Moreover, it should also be noted that in setting initial conditions final converged solution should be independent of the flow initialization.

On the other hand, boundary conditions are necessary to obtain a unique and accurate solution. The correct implementation of the boundary condition is one of the most important aspects of every flow solver. In addition to the accuracy of the solution, the robustness and convergence speed are considerably influenced by the proper implementation of the boundary conditions [1]. In this study, characteristic type boundary conditions are used and will be presented in this chapter.

4.1   INITIAL CONDITIONS

In this study initials conditions are set as freestream values of pressure, density and velocity (given as Mach number and angle of attack) in the whole computational domain which is a common approach in external aerodynamics [1].

Therefore by using the input Mach number, components of the conserved vector variables are set as follows:

$$
U = \begin{bmatrix} \rho \\ \\ \rho u \\ \\ \rho v \\ \\ e \end{bmatrix} = \begin{bmatrix} \rho_{total}\left(1+\dfrac{\gamma-1}{2}M_{far}^2\right)^{\frac{-1}{\gamma-1}} \\ \\ \rho_{total}\,a_{total}\cos\alpha_1\left(1+\dfrac{\gamma-1}{2}M_{far}^2\right)^{\frac{-(\gamma-1)}{2(\gamma-1)}} \\ \\ \rho_{total}\,a_{total}\cos\alpha_2\left(1+\dfrac{\gamma-1}{2}M_{far}^2\right)^{\frac{-(\gamma-1)}{2(\gamma-1)}} \\ \\ \left(\dfrac{p_{total}}{\gamma-1}+\dfrac{1}{2}\rho_{total}a_{total}^2M_{far}^2\right)\left(1+\dfrac{\gamma-1}{2}M_{far}^2\right)^{\frac{-\gamma}{2(\gamma-1)}} \end{bmatrix}
\qquad (4.1)
$$

For the turbulence models, the free stream values of turbulence parameters, which are used to initialize the flow field, are taken as follows:

$$
\tilde{v}_\infty = 0.1 * v_\infty \qquad (4.2)
$$

$$
\overline{Re}_\infty = 0.1 \qquad (4.3)
$$

4.2   IMPLEMENTATION OF BOUNDARY CONDITIONS

The characteristic type boundary conditions, which are used in this study, are implemented by using the predictor-corrector method. In this method, conservative variables of the nodes on the boundaries are updated according to the Lax-Wendroff in the predictor step. On the other hand, in the corrector step, the characteristic type boundary conditions are applied explicitly by using the predicted values at the boundary nodes. The solution is updated as follows:

$$\delta U_{boundary} = U_{corrected} - U_{predicted} \qquad (4.4)$$

In the above formulation, $U_{predicted}$ term stands for the predicted conservative variable which is obtained from the solution of Lax-Wendroff method and the $U_{corrected}$ term stands for the corrected conservative variables.

4.3 CHARACTERISTIC TYPE BOUNDARY CONDITIONS

In order to derive the characteristic type boundary conditions, the Euler equations are written in terms of primitive variables in the normal and tangential directions at a boundary as follows:

$$\frac{\partial \tilde{U}}{\partial t} + \frac{\partial \tilde{F}}{\partial n} + \frac{\partial \tilde{G}}{\partial s} = 0 \qquad (4.5)$$

where n and s denotes the local coordinates in the normal and tangential directions, respectively. Assuming that variations in the normal direction is larger than the tangential direction, so the derivatives in tangential direction can be dropped from Equation (4.5) to get the following form [15]

$$\frac{\partial \tilde{U}}{\partial t} + \frac{\partial \tilde{F}}{\partial n} = 0 \qquad (4.6)$$

it can also be expressed in quasi-linear form as follows:

$$\frac{\partial \tilde{U}}{\partial t} + \tilde{A} \frac{\partial \tilde{U}}{\partial n} = 0 \qquad (4.7)$$

In above equation $\tilde{U}$ stands for the primitive variable vector and $\tilde{A}$ stands for the Jacobian matrix term, and these terms can be given as follows:

56

$$\tilde{U} = \begin{bmatrix} \rho \\ u_n \\ u_s \\ p \end{bmatrix} \tag{4.8}$$

and

$$\tilde{A} = \begin{bmatrix} \bar{u}_n & \bar{\rho} & 0 & 0 \\ 0 & \bar{u}_n & 0 & \dfrac{1}{\rho} \\ 0 & 0 & \bar{u}_n & 0 \\ 0 & \overline{\rho c}^{\,2} & 0 & \bar{u}_n \end{bmatrix} \tag{4.9}$$

where u_n and u_s correspond to normal and tangential velocity vector components respectively and c represents the speed of sound. The barred quantities in the Jacobian matrix $\tilde{A}$ are averaged values and taken as constants.

The Jacobian matrix $\tilde{A}$ can be diagonalized by using matrix L as follows:

$$L^{-1}\tilde{A}\,L = \Lambda \tag{4.10}$$

where

$$L = \begin{bmatrix} 1 & 0 & \dfrac{\rho}{2\bar{c}} & \dfrac{\rho}{2\bar{c}} \\ 0 & 0 & \dfrac{1}{2} & \dfrac{1}{-2} \\ 0 & -1 & 0 & 0 \\ 0 & 0 & \dfrac{\bar{\rho}}{2\bar{c}} & \dfrac{\bar{\rho}}{2\bar{c}} \end{bmatrix} \tag{4.11a}$$

and

$$L^{-1} = \begin{bmatrix} 1 & 0 & 0 & -\dfrac{1}{c^2} \\ 0 & 0 & -1 & 0 \\ 0 & 1 & 0 & \dfrac{1}{\overline{\rho c}} \\ 0 & -1 & 0 & \dfrac{1}{\overline{\rho c}} \end{bmatrix}$$ (4.11b)

Equation (4.10) yields the diagonal matrix Λ is obtained

$$\Lambda = \begin{bmatrix} \overline{u}_n & 0 & 0 & 0 \\ 0 & \overline{u}_n & 0 & 0 \\ 0 & 0 & \overline{u}_n + \overline{c} & 0 \\ 0 & 0 & 0 & \overline{u}_n - \overline{c} \end{bmatrix}$$ (4.12a)

which can also be expressed as follows:

$$\Lambda = \begin{bmatrix} \lambda_1 & 0 & 0 & 0 \\ 0 & \lambda_2 & 0 & 0 \\ 0 & 0 & \lambda_3 & 0 \\ 0 & 0 & 0 & \lambda_4 \end{bmatrix}$$ (4.12b)

In the above formulation $\lambda_1, \lambda_2, \lambda_3$ and λ_4 are the eigenvalues of the Jacobian matrix $\tilde{A}$. Jacobian matrix $\tilde{A}$ can also be expressed as

$$\tilde{A} = L\Lambda L^{-1}$$ (4.13)

By substituting Equation (4.13) into Equation (4.7) following result can be obtained

$$\frac{\partial \tilde{U}}{\partial t} + L\Lambda L^{-1} \frac{\partial \tilde{U}}{\partial n} = 0$$ (4.14)

58

The above formulation can be left multiplied by L^{-1} to obtain

$$L^{-1}\frac{\partial \tilde{U}}{\partial t} + \Lambda L^{-1}\frac{\partial \tilde{U}}{\partial n} = 0 \tag{4.15}$$

The characteristic variable vector can be defined as follows:

$$\delta W = L^{-1}\delta \tilde{U} \tag{4.16}$$

Substituting Equation (4.16) into Equation (4.15) , one can obtain following equation

$$\frac{\partial W}{\partial t} + \Lambda \frac{\partial W}{\partial n} = 0 \tag{4.17}$$

where W is the vector of linearized characteristic variables and can be written as follows:

$$W = \begin{bmatrix} \rho - \dfrac{p}{c^2} \\ -u_s \\ u_n + \dfrac{p}{c^2} \\ -u_n + \dfrac{p}{c^2} \end{bmatrix} \tag{4.18}$$

For the implementation both physical and numerical types of boundary conditions are used. Type of boundary condition used in this study depends on the eigenvalues of the characteristic. For the positive eigenvalues, which means that the characteristics are entering the flow domain from outside, the physical boundary conditions are used and far field values are assigned as corrected value. On the other hand for the negative and zero eigenvalues, which means that the characteristic are moving outside the domain, numerical boundary conditions are used. In this case, the result of numerical scheme is used as corrected value [10, 15].

The physical boundary conditions can be expressed by using the non-reflective boundary conditions, so that the local perturbations propagated along incoming characteristics must be vanished [19]. As a result of this statement,

$$\frac{\partial W}{\partial t} = 0 \tag{4.19}$$

or

$$\Lambda \frac{\partial W}{\partial n} = 0 \tag{4.20}$$

The above equation can be applied as follows

$$\Delta W = 0 \tag{4.21}$$

Details of boundary condition implementation which depends on the eigenvalues are given in following sections:

4.3.1 Subsonic Inlet

For the case of subsonic inlet, $c > u_n > 0$ so the eigenvalues $\lambda_1, \lambda_2, \lambda_3$ are positive and λ_4 is negative. So the fourth characteristic variable has to be determined from the interior domain and the other three physical boundary conditions are to be specified at the boundary.

$$\Delta W_1 = 0 \Rightarrow \qquad \rho_{corrected} - \frac{p_{corrected}}{c^2} = \rho_{far} - \frac{p_{far}}{c^2} \tag{4.22a}$$

$$\Delta W_2 = 0 \Rightarrow \qquad u_{s,corrected} = u_{s,far} \tag{4.22b}$$

$$\Delta W_3 = 0 \Rightarrow \qquad u_{n,corrected} + \frac{p_{corrected}}{\overline{\rho c}} = u_{n,far} + \frac{p_{far}}{\overline{\rho c}} \qquad (4.22c)$$

$$\Delta W_4 = 0 \Rightarrow \qquad -u_{n,corrected} + \frac{p_{corrected}}{\overline{\rho c}} = -u_{n,predicted} + \frac{p_{predicted}}{\overline{\rho c}} \qquad (4.22d)$$

In the above formulations, the subscript *corrected* stands for the corrected value and the subscript *predicted* stands for the value predicted by Lax-Wendroff scheme. Solving the above set of equations for the corrected primitive variables, one can obtain

$$p_{corrected} = \frac{1}{2} \left[p_{far} + p_{predicted} + \overline{\rho c} \left(u_{n,far} - u_{n,predicted} \right) \right] \qquad (4.23a)$$

$$\rho_{corrected} = \rho_{far} + \frac{p_{corrected} - p_{far}}{\overline{c}^2} \qquad (4.23b)$$

$$u_{n,corrected} = u_{n,far} + \frac{p_{far} - p_{corrected}}{\overline{\rho c}} \qquad (4.23c)$$

$$u_{s,corrected} = u_{s,far} \qquad (4.23d)$$

Finally, for the Spalart-Allmaras and Baldwin-Barth model free stream values are used

$$\tilde{v} = v_{\infty} \qquad (4.24)$$

$$\overline{Re}_t = Re_{t\infty} \qquad (4.25)$$

4.3.2 Supersonic Inlet

In this case $u_n > c$, as a result all the eigenvalues $\lambda_1, \lambda_2, \lambda_3, \lambda_4$ are positive and all the characteristic values are corrected using the free stream values.

$$\Delta W_1 = 0 \Rightarrow \qquad \rho_{corrected} - \frac{p_{corrected}}{\bar{c}^2} = \rho_{far} - \frac{p_{far}}{\bar{c}^2} \qquad (4.26a)$$

$$\Delta W_2 = 0 \Rightarrow \qquad u_{s,corrected} = u_{s,far} \qquad (4.26b)$$

$$\Delta W_3 = 0 \Rightarrow \qquad u_{n,corrected} + \frac{p_{corrected}}{\rho c} = u_{n,far} + \frac{p_{far}}{\rho c} \qquad (4.26c)$$

$$\Delta W_4 = 0 \Rightarrow \qquad -u_{n,corrected} + \frac{p_{corrected}}{\rho c} = -u_{n,far} + \frac{p_{far}}{\rho c} \qquad (4.26d)$$

Solving above set of equation for primitive variables the following set of equations can be obtained

$$p_{corrected} = p_{far} \qquad (4.27a)$$

$$\rho_{corrected} = \rho_{far} \qquad (4.27b)$$

$$u_{n,corrected} = u_{n,far} \qquad (4.27c)$$

$$u_{s,corrected} = u_{s,far} \qquad (4.27d)$$

Finally, it should be noted that, the supersonic inlet boundary conditions used for the Spalart-Allmaras and Baldwin-Barth turbulence models are just the same as the ones in the subsonic case.

4.3.3 Subsonic Exit

In the case of subsonic outflow, $u_n < 0$ and $|u_n| < \bar{c}$. As a consequence, λ_4 is positive, and $\lambda_{1,}, \lambda_2, \lambda_3$ are negative. Therefore, only one physical boundary condition will be imposed which corresponds to W_4

$$\Delta W_1 = 0 \Rightarrow \quad \rho_{corrected} - \frac{p_{corrected}}{\bar{c}^2} = \rho_{predicted} - \frac{p_{predicted}}{\bar{c}^2} \tag{4.28a}$$

$$\Delta W_2 = 0 \Rightarrow \quad u_{s,corrected} = u_{s,predicted} \tag{4.28b}$$

$$\Delta W_3 = 0 \Rightarrow \quad u_{n,corrected} - \frac{p_{corrected}}{\overline{\rho c}} = u_{n,far} - \frac{p_{far}}{\overline{\rho c}} \tag{4.28c}$$

$$\Delta W_4 = 0 \Rightarrow \quad -u_{n,corrected} + \frac{p_{corrected}}{\overline{\rho c}} = -u_{n,predicted} + \frac{p_{predicted}}{\overline{\rho c}} \tag{4.28d}$$

By solving above set of equations for corrected values, the following terms can be obtained

$$p_{corrected} = p_{far} \tag{4.29a}$$

$$\rho_{corrected} = \rho_{predicted} + \frac{p_{corrected} - p_{predicted}}{\bar{c}^2} \tag{4.29b}$$

$$u_{n,corrected} = u_{n,predicted} + \frac{p_{corrected} - p_{predicted}}{\overline{\rho c}} \tag{4.29c}$$

$$u_{s,corrected} = u_{s,predicted} \tag{4.29d}$$

Finally, at the exit, a first order extrapolation is used for the turbulence models. Hence for Spalart-Allmaras and Baldwin-Barth models:

$$\tilde{v}_{i,j} = 2\,\tilde{v}_{i+1,j} - \tilde{v}_{i+2,j} \tag{4.30}$$

$$\overline{Re}_{t\,i,j} = 2\,\overline{Re}_{t\,i+1,j} - \overline{Re}_{t\,i+2,j} \tag{4.31}$$

4.3.4 Supersonic Exit

In this case of supersonic outflow, $u_n < 0$. As a result of this all the eigenvalues become negative. No physical boundary conditions are used:

$$\Delta W_1 = 0 \Rightarrow \qquad \rho_{corrected} - \frac{p_{corrected}}{\bar{c}^2} = \rho_{predicted} - \frac{p_{predicted}}{\bar{c}^2} \tag{4.32a}$$

$$\Delta W_2 = 0 \Rightarrow \qquad u_{s,corrected} = u_{s,predicted} \tag{4.32b}$$

$$\Delta W_3 = 0 \Rightarrow \qquad u_{n,corrected} + \frac{p_{corrected}}{\overline{\rho c}} = u_{n,predicted} + \frac{p_{predicted}}{\overline{\rho c}} \tag{4.32c}$$

$$\Delta W_4 = 0 \Rightarrow \qquad -u_{n,corrected} + \frac{p_{corrected}}{\overline{\rho c}} = -u_{n,predicted} + \frac{p_{predicted}}{\overline{\rho c}} \tag{4.32d}$$

By solving above set of equations, one can obtain following conditions

$$p_{corrected} = p_{far} \tag{4.33a}$$

$$\rho_{corrected} = \rho_{predicted} \tag{4.33b}$$

$$u_{n,corrected} = u_{n,predicted} \qquad (4.33\text{c})$$

$$u_{s,corrected} = u_{s,predicted} \qquad (4.33\text{d})$$

For the Spalart-Allmaras and Baldwin-Barth turbulence models, the same first order extrapolation procedure, carried out for the subsonic exit, is used.

4.4   SYMMETRY BOUNDARY CONDITION

In the symmetry boundary condition, the flow velocity is tangent to the surface. Therefore normal component of the velocity is set to zero on the boundary which means $u_{n,wall} = 0$. As a result $\lambda_1, \lambda_2, \lambda_3$ are negative and λ_4 positive. Therefore,

$$\Delta W_1 = 0 \Rightarrow \qquad \rho_{corrected} - \frac{p_{corrected}}{\bar{c}^2} = \rho_{predicted} - \frac{p_{predicted}}{\bar{c}^2} \qquad (4.34\text{a})$$

$$\Delta W_2 = 0 \Rightarrow \qquad u_{s,corrected} = u_{s,predicted} \qquad (4.34\text{b})$$

$$\Delta W_3 = 0 \Rightarrow \qquad u_{n,corrected} - \frac{p_{corrected}}{\overline{\rho c}} = u_{n,wall} - \frac{p_{wall}}{\overline{\rho c}} \qquad (4.34\text{c})$$

$$\Delta W_4 = 0 \Rightarrow \qquad -u_{n,corrected} + \frac{p_{corrected}}{\overline{\rho c}} = -u_{n,predicted} + \frac{p_{predicted}}{\overline{\rho c}} \qquad (4.34\text{d})$$

The results obtained for corrected values can be stated as follows:

$$u_{n,corrected} = u_{n,wall} = 0 \qquad (4.35\text{a})$$

$$u_{s,corrected} = u_{s,predicted} \qquad (4.35\text{b})$$

$$p_{corrected} = p_{predicted} - \rho\bar{c}u_{n,predicted} \qquad (4.35\text{c})$$

$$\rho_{corrected} = \rho_{predicted} + \frac{p_{corrected} - p_{predicted}}{\bar{c}^2} \qquad (4.35d)$$

and for the turbulence models both for Spalart-Allmaras and Baldwin-Barth, a first order extrapolation is used:

$$\tilde{v}_{i,j} = \tilde{v}_{i,j\pm1}$$

$$(4.36)$$

$$\overline{Re}_{t_{i,j}} = \overline{Re}_{t_{i,j\pm1}}$$

4.5   SOLID WALL BOUNDARY CONDITION

This type of boundary condition is also called the no-slip boundary condition. In this study all the solid walls are considered stationary. Therefore

$$u = v = 0 \qquad (4.37)$$

In this study, adiabatic boundary condition is used, that is, heat flux on the wall is set to zero.

$$\frac{\partial T}{\partial n} = 0 \qquad (4.38)$$

In the normal direction to the solid boundary, using boundary layer assumptions, y-momentum equation reduces to

$$\frac{\partial p}{\partial n} = 0 \qquad (4.39)$$

For the Spalart-Allmaras and Baldwin-Barth models solid wall boundary conditions are taken as zero [12, 11].

$$\tilde{v} = 0 \tag{4.40}$$

$$\overline{Re}_t = 0 \tag{4.41}$$

4.6   FAR FIELD BOUNDARY CONDITION

In far field boundary condition, the propagating waves should neither be reflected nor emitted. In order to implement on ideal far field condition, the boundary should be placed sufficiently far, say 50-60 or sometimes 100 characteristic lengths away [17], [18].Practical approach is to put the far field boundary closer, say 5 – 6 characteristic lengths away, but directly imposing the free stream values causes the reflection of these waves in non-physical manner from the far field boundaries. Viscous mechanism of the Navier-Stokes equations is generally able to dissipate these waves provided that the far field boundary is placed far enough from the solid body [16]. There are also other methods to reduce the effect of reflection of the waves, one of these methods is suggested by Hirsch [19] .In this method special corrections based on lift coefficient are added to the free stream values and corrected values are found [15]. However, in this study, the free stream values of primitive variables are directly imposed on the far field boundaries without any change.

CHAPTER 5

RESULTS AND DISCUSSIONS

Performance and accuracy of the turbulence models implemented into the Navier-Stokes solver is tested on various test cases. These test cases include transonic flow over NACA 0012 airflow and turbulent flow over flat plate

Validity and accuracy of Navier-Stokes solver is also verified. For this purpose the laminar flat plate problem is chosen. Laminar flat plate test case for a Navier-Stokes solver is one of the best test cases since the dominant forces are viscous terms in a flat plate problem and viscous terms can be verified [16]. In this test case, a free stream Mach number of 0.3 and a free stream Reynolds number of 35000 are selected.

The next test case is the turbulent flow over a flat plate with a free stream Reynolds number of 6,000,000 and a Mach number of 0.3. In this case, the transition point is fixed and specified. Both Spalart-Allmaras and Baldwin-Barth turbulence models are tested. The numerical results are compared with the analytical solution.

The final test case belongs to transonic flow over the NACA 0012. This test case is handled in Reynolds number of 9,000,000 with an angel of attack 2.26 and free stream Mach number of 0.799. Both Spalart-Allmaras and Baldwin-Barth turbulence models are tested. The numerical results are compared with the numerical solution of Tınaztepe [10] and experimental results.

5.1 LAMINAR FLOW OVER FLAT PLATE

The main purpose of this test case is to check the validity and performance of the Navier–Stokes solver in which turbulence models will be implemented. For this purpose the laminar flow over flat plate problem is chosen, which is the best way to check whether the solver handles the viscous terms correctly or not. In this test case free stream Mach number of 0.3 and Reynolds number of 35000 is chosen. In this kind of test case, pressure gradient is zero except the region closed to the leading edge. Therefore, the grid is clustered in horizontal direction at the leading edge for 121x81 H type structured grid, which is shown in Figure 5.1.
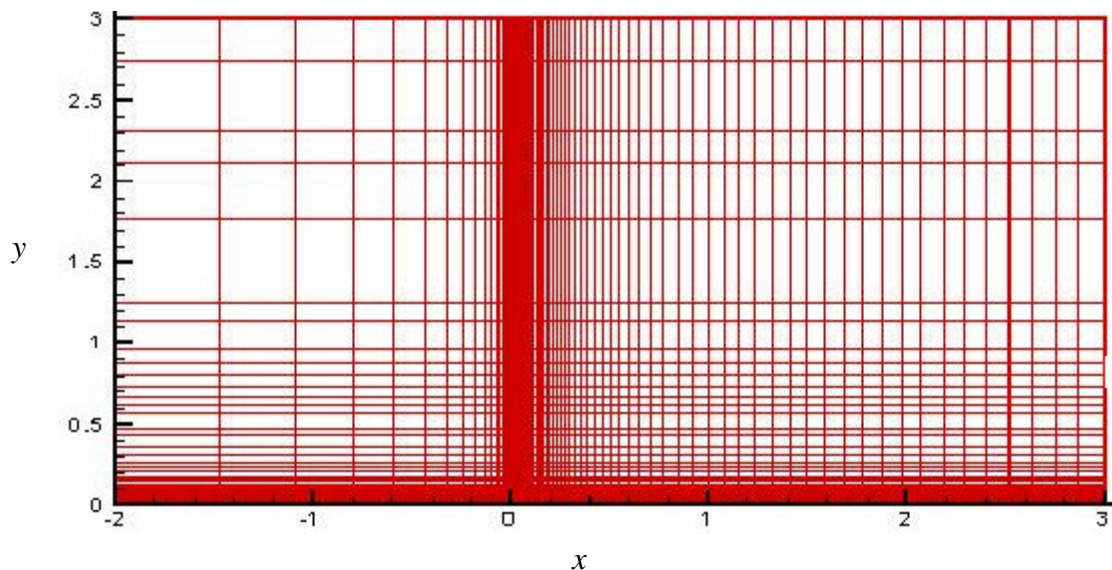
Figure 5.1 H type Grid for Laminar Flat Plate Test Case

The minimum Δx used in the clustering is 0.0005. In order to get sufficient accuracy, the grid is also highly clustered near flat plate in y direction; the minimum Δy used is 0.00022 of the cord length so that there are more than 20 points in the boundary layer. In the upwind direction of this grid, there are 30 nodes on the slip surface, 70 nodes on the flat plate and 21 nodes in the wake region.

In this test case, during the solution, second order-smoothing coefficient of 0.001 and CFL number of 0.5 is taken. The velocity profiles at location of 60% of the cord and local skin friction coefficient are compared with Blasius solution. The local skin friction coefficient, C_f is calculated by using following formula:

$$C_f = \frac{\tau_w}{\frac{1}{2}\rho_\infty U_\infty^2}$$

(5.1)

where ρ_∞, U_∞ are free stream values for density and velocity respectively, and τ_w is the value of wall friction calculated locally on the flat plate. Blasius exact solution for the local skin friction coefficient, C_f is given as

$$C_f = 0.664(Re_x)^{-0.5}$$

(5.2)

where Re_x is the Reynolds number at position x on the plate and can be defined as follows:

$$Re_x = \frac{\rho_\infty U_\infty x}{\mu_\infty}$$

(5.3)

Obtained results for tangential velocity profile, normal velocity profile and the local skin friction distribution are presented in Figures 5.2, 5.3 and 5.4 respectively. As shown in Figures 5.2 and 5.3 results obtained for tangential velocity and normal velocity profiles are acceptable since there not much deviations from the Blasius solution in both figures. But however there is slight deviation for the local skin friction distribution at the leading edge, which is presented in Figures 5.4. This kind of discrepancy near the leading edge is expected, since the Blasius solution uses the boundary layer assumptions and the flow near the leading edge does not satisfy the boundary layer assumptions. In fact the flow near the leading edge can only be modeled correctly by using the full Navier-Stokes equations. As a result of this fact, the overall accuracy of the Navier-Stokes solver is acceptable.
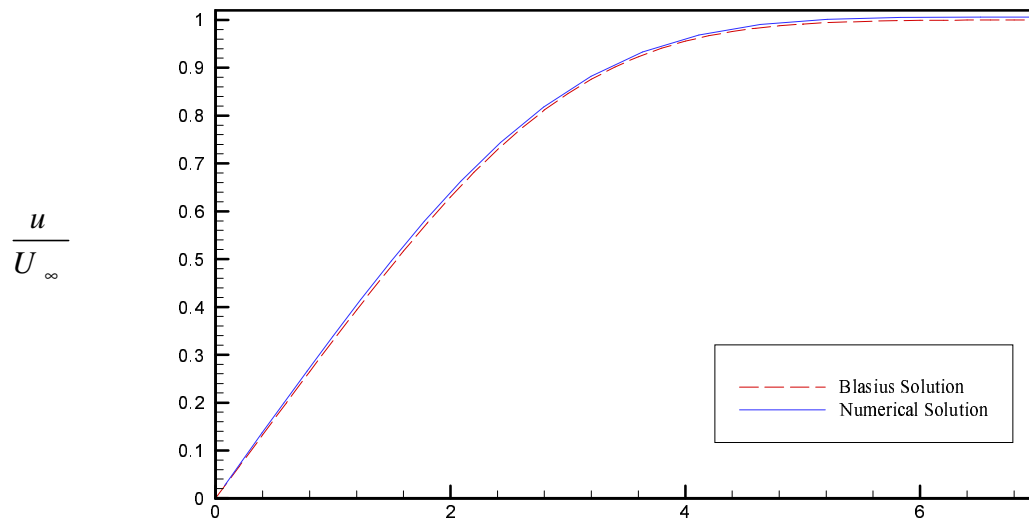
$$\eta = \frac{y}{x}\sqrt{\text{Re}_x}$$

Figure 5.2 Tangential Velocity Profiles.
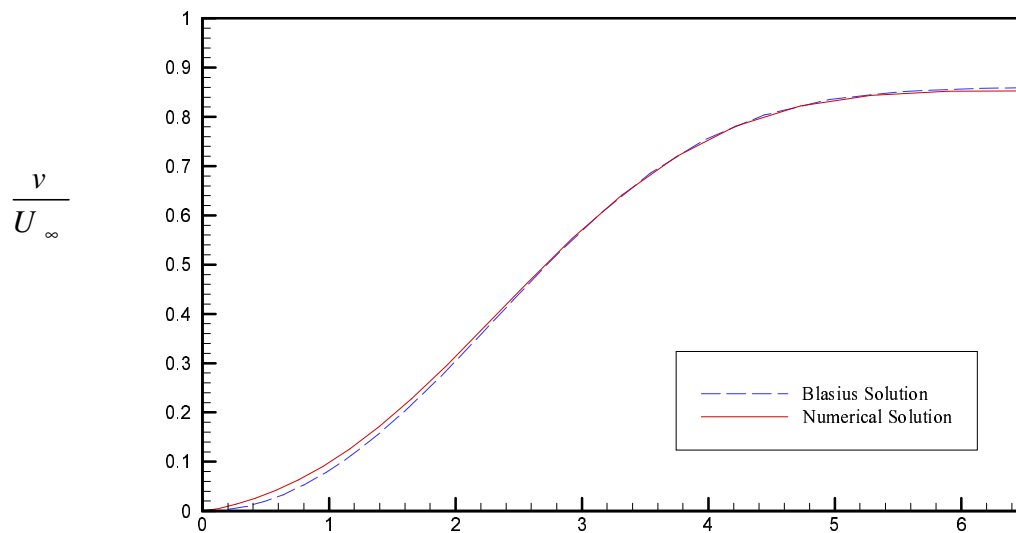
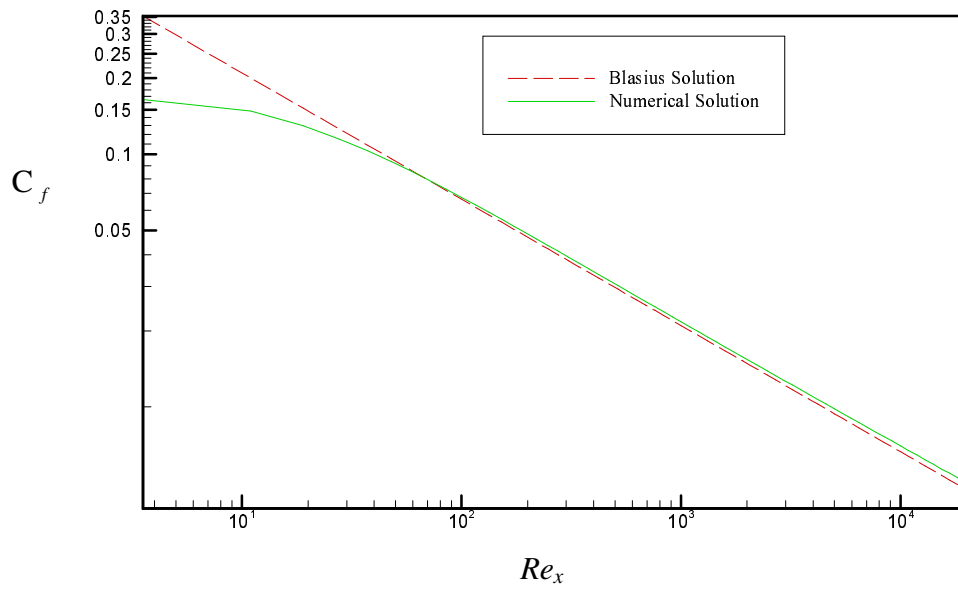$$\eta = \frac{y}{x}\sqrt{\text{Re}_x}$$

Figure 5.3 Normal Velocity Profiles.

Figure 5.4 Local Skin Friction Coefficient.

5.2   TURBULENT FLOW OVER FLAT PLATE

In this test case both Spalart-Allmaras and Baldwin-Barth turbulence models are tested. For this test case 121x81 H grid is used. Grid, which is shown in Figure 5.5, is clustered at both leading and trailing edge with minimum Δy of 0.000015 and minimum Δx of 0.000032. Besides this, grid consists of 37 nodes in the upstream region, 70 nodes on the flat plate, and 8 nodes in the wake region.
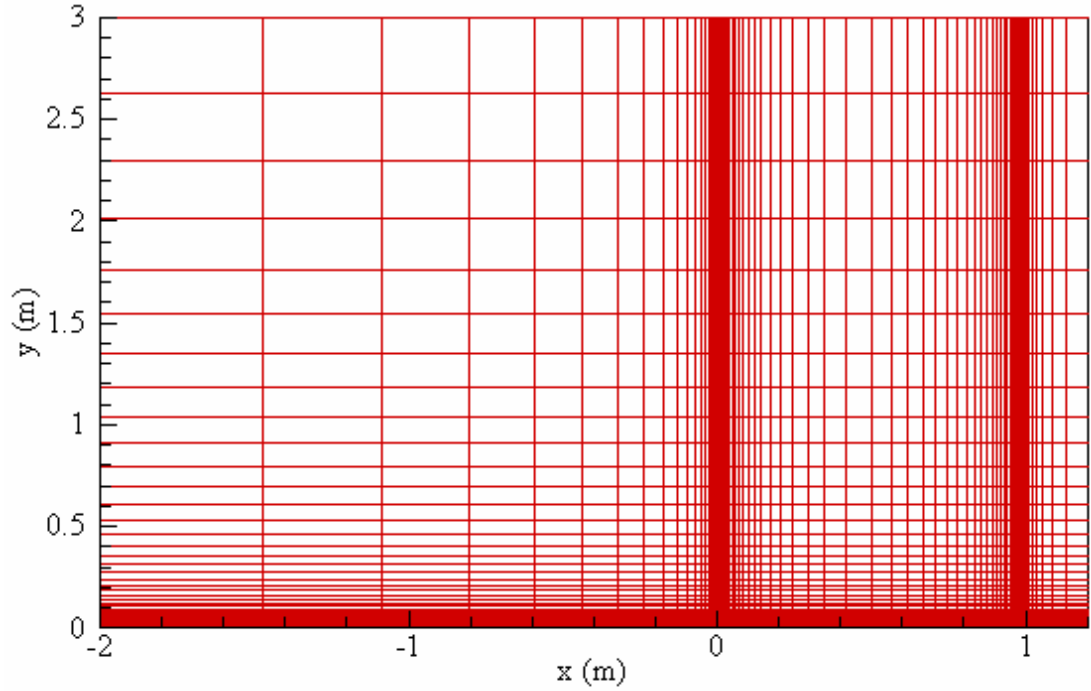
Figure 5.5   Grid Used for the Turbulent Flat Plate Problem.

For this test case, in order to be consistent with researchers [16, 17, and 18], a free stream Mach number of 0.3 and a Reynolds number of 6,000,000 is chosen. Moreover transition to turbulence is taken at fixed point which is 0.054 m from leading edge which corresponds to a Reynolds number of 324,000.

In order to check the accuracy of the models, both empirical and analytical methods are used. For local skin friction, Blasius exact solution, which is given in Equation (5.2), is used for laminar flow regime and Prandtl's 1/5 law is used for the turbulent flow region. Prandtl's 1/5 law is given as follows:

$$C_f = 0.0592(\mathrm{Re}_x)^{-0.2} \tag{5.4}$$

On the other hand calculated turbulent velocity profiles are compared with the empirically obtained universal velocity distributions. For the turbulent non-dimensional velocity profiles the following formula is used:

$$u^+ = \begin{cases} y^+ & , \quad 0 < y^+ < 5 \\ 5.0\log(y^+) - 3.05, & 5 < y^+ < 30 \\ 2.5\log(y^+) + 5.5 \;, & 30 < y^+ \end{cases} \tag{5.5}$$

where y^+ is defined in Equation (2.27d) and non-dimensional velocity u^+ can be given as follows:

$$u^+ = \frac{u}{u_\tau} \tag{5.6}$$

where u_τ is friction velocity given in Equation (2.27e).

5.2.1. Spalart-Allmaras Model

Having implemented Spalart-Allmaras model, stability of the numerical work is maintained by increasing the second order artificial smoothing coefficient. So during discretization of the Spalart-Allmaras model for both finite difference and coupled cases second order artificial smoothing coefficient is increased. Therefore second order artificial smoothing coefficient for uncoupled discretization of the model is increased from 0.001 to 0.3. Moreover, it is increased from 0.001 to 0.41 for coupled discretization. Consequently, an additional equation is solved with the Navier-Stokes equation and in order to increase the stability, artificial damping factor increased more. For both cases CFL number is taken as 0.5.

Numerical results obtained from Spalart-Allmaras model are shown in Figures 5.6, 5.7 and 5.8. As seen in Figure 5.6, coupled solution predicts the skin friction coefficient quite well. On the other hand finite difference discretization of turbulence model underpredicts the local skin friction coefficient just before transition. This kind of deviation may result of the discretization of the model in finite difference domain since coupled solution give better prediction. It should also be noted that velocity profiles deviate from universal velocity distribution at the end

of the boundary layer. This kind of deviation in the outer boundary layer is reasonable and it is also observed in experimental results [15]. But overall solutions are in good agreement with analytical solutions.
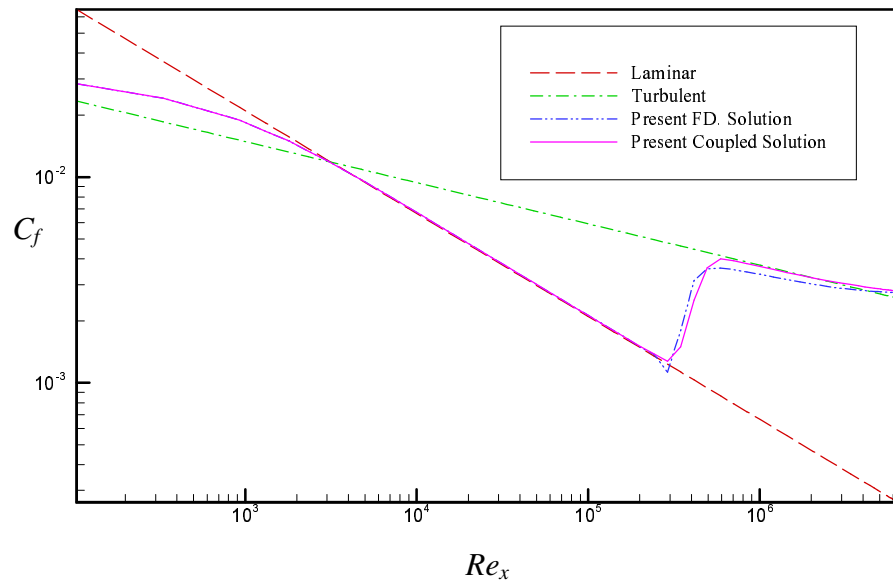

Figure 5.6   Local Skin Friction Coefficients along the Flat Plate Obtained by Spalart-Allmaras Model.
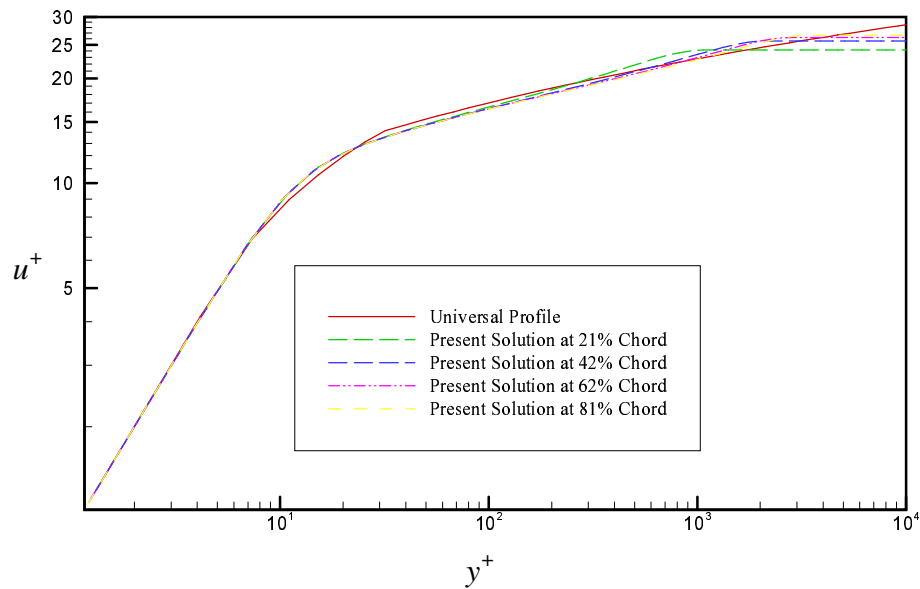

Figure 5.7   Non-dimensional Turbulent Velocity Profiles Obtained by Spalart-Allmaras Model with Coupled Solution.
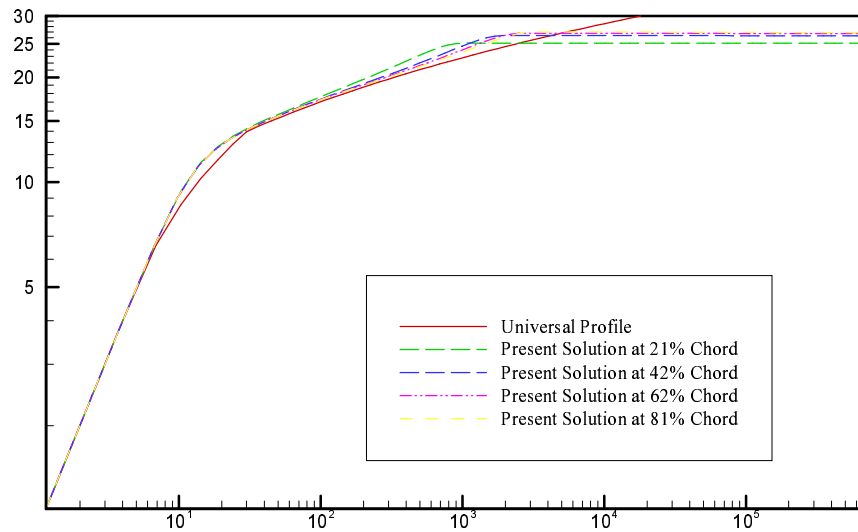
Figure 5.8   Non-dimensional Turbulent Velocity Profiles Obtained by
                 Spalart-Allmaras Model with Finite Difference Solution

5.2.2   Baldwin Barth Turbulence Model

For Baldwin-Barth turbulence model second order artificial smoothing coefficient is taken as 0.3 which is the same as the one chosen for Spalart-Allmaras turbulence model. CFL number is chosen as 0.5, which again the same as the one is chosen for Spalart-Allmaras model. The local skin friction distribution over flat-plate and turbulent velocity profiles are given in Figures 5.9 and 5.10 respectively. In Figure 5.9, it is seen that the local skin friction distribution is underpredicted before the transition, when compared with the analytical result. This deviation may be in consequence of the model's interaction with the laminar part of the flow. This kind of deviation is also observed by references [17, 18] in local skin friction distribution of $k - \varepsilon$ two equation turbulence model and Baldwin-Barth turbulence model is derived from $k - \varepsilon$ turbulence model. Since this deviation is reasonable and velocity profile is in good agreement with universal profile, overall result is acceptable.
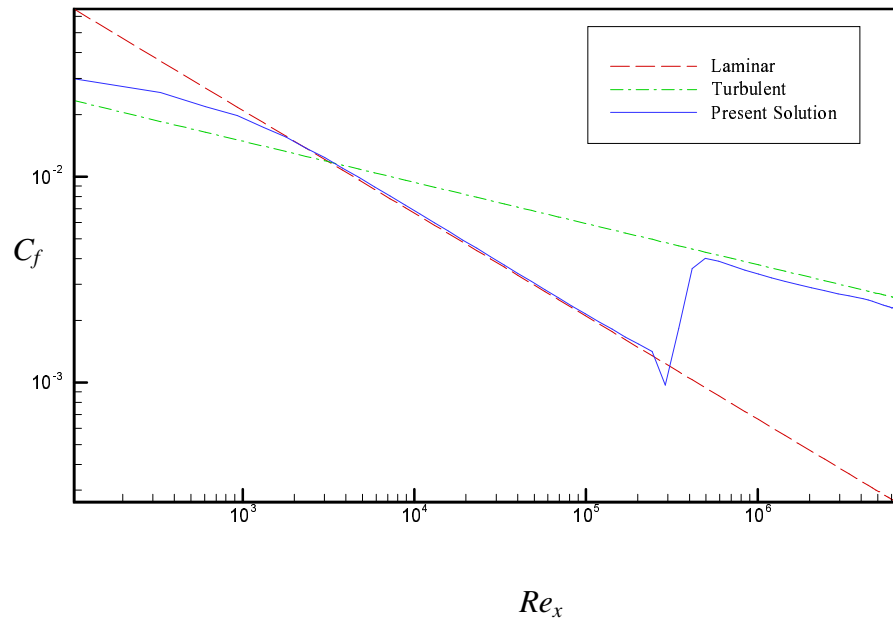
76

Figure 5.9   Local Skin Friction Coefficient Along the Flat Plate Obtained by Baldwin-Barth Model
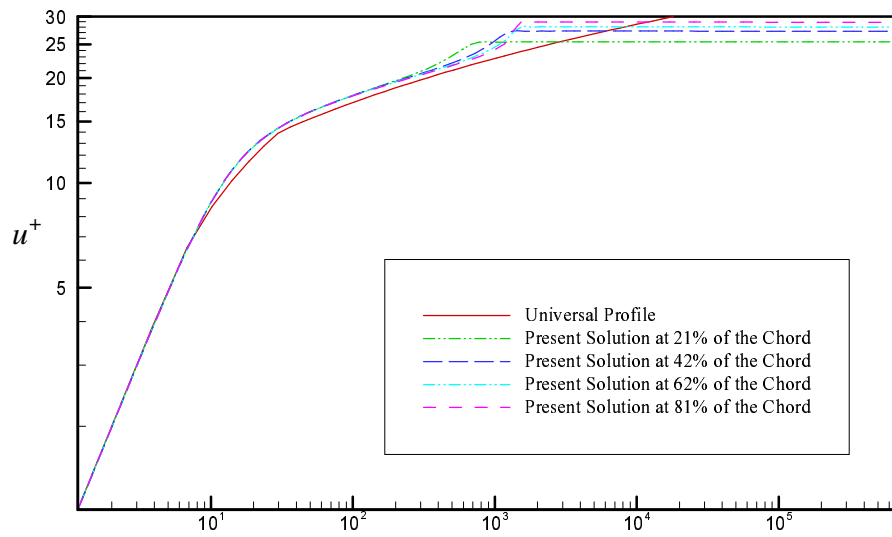

Figure 5.10   Non-dimensional Turbulent Velocity Profiles Obtained by Baldwin-Barth model

5.2.3. Comparison of the Turbulence Models Over Turbulent Flat Plate

Local skin friction distribution over turbulent flat plate of both one equation turbulence models and Baldwin-Lomax turbulence model [18] are compared in Figure 5.11. As it can be seen from Figure 5.11 that among the one equation turbulence models, the best prediction of the local skin friction distribution is obtained by Spalart-Allmaras turbulence model with coupled solution. Finite difference solution of both Baldwin-Barth and Spalart-Allmaras turbulence models underpredict when they are compared with analytical solution. Both of the finite difference solutions of the turbulence models have a deviation in downward direction just before the transition. In Figure 5.11 more deviation can be observed in Baldwin-Barth turbulence model then Spalart-Allmaras turbulence model. For Baldwin-Barth solution this deviation may be due to the models interaction with laminar part of the flow [15, 18]. But for the Spalart-Allmaras turbulence model, this deviation is thought to be due to the discretization of the model in finite difference method. On the other hand, it can be observed from Figure 5.11 the best solution is obtained by the Baldwin-Lomax turbulence model. Infact zero equation models require less amount of computational effort, it is one of the advantageous for this kind of flow where small amount of adverse pressure gradient is present [18].

In Figure 5.12 turbulent velocity profiles of one equation models and universal velocity distributions are plotted together. As it can be observed, both models give similar solutions and they are in good agreement with empirical results.

Finally, x-momentum averaged residuals are given in Figure 5.13. Solutions of the models are allowed to continue until the solver run for 65,000 iterations. Number of iterations are enough for convergence of the both turbulence models.
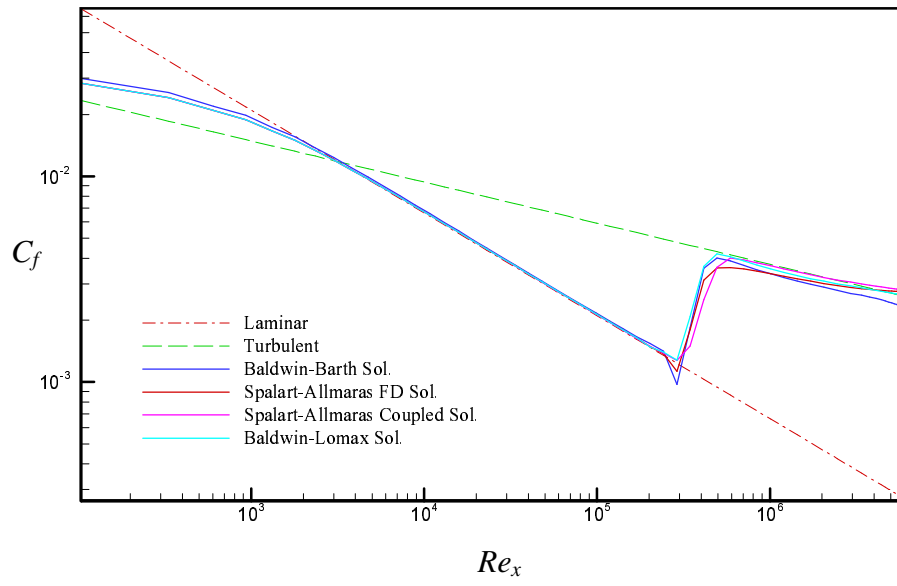
Figure 5.11   Comparison of Local Skin friction Distributions of the Turbulence Models in Turbulent Flat Plate Problem
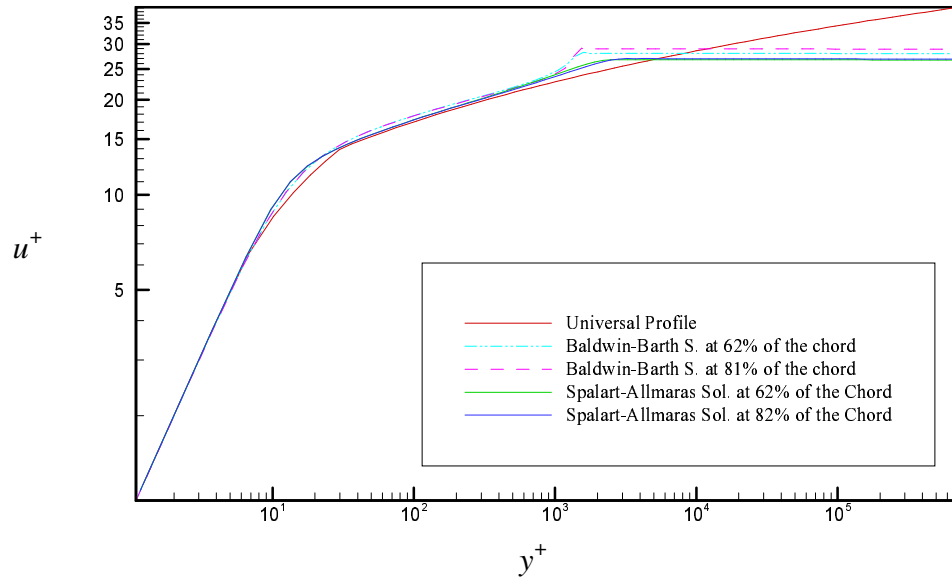

Figure 5.12   Comparison of Non Dimensional Velocity Profiles Obtained from Both of the Turbulence Models in Turbulent Flat Plate Problem
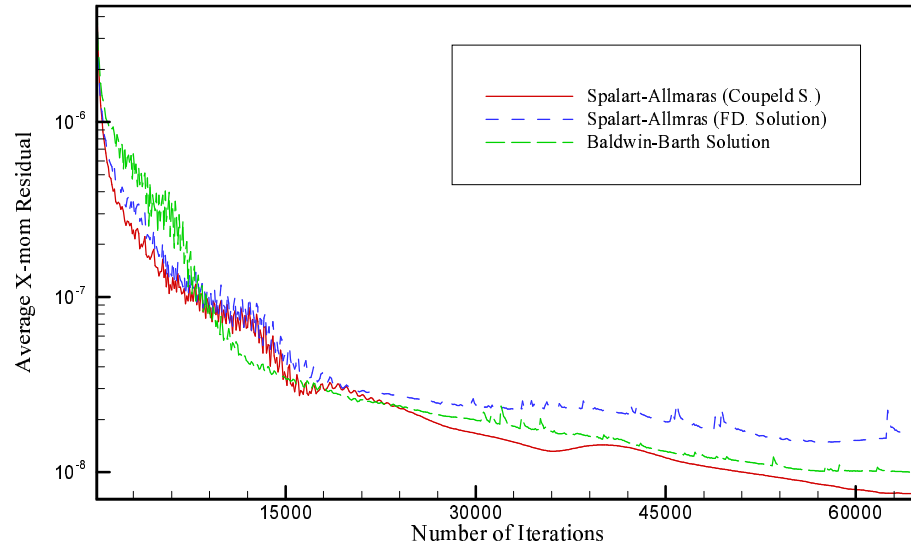
79

Figure 5.13   Residual History of the Turbulence Models

5.3   TURBULENT TRANSONIC FLOW OVER NACA-0012 AIRFOIL

Transonic flow occurs when there is a mixed of subsonic and supersonic flow in the same flow field and usually the supersonic part of the flow is terminated by a shock wave [20]. This makes the case very challenging and a good test case for the computational research.

In this test case, turbulent transonic flow over NACA 0012 airfoil is investigated. Transonic flow turbulent flow with a free stream Reynolds number of 9,000,000 is considered. This test case is handled by other researchers like Baldwin-Barth[9] and Tınaztepe [15]. Performance of the models and solver are checked for the free stream Mach number of 0.799 with an angle of attack 2.26 degree. In this test case CFL number and second order artificial smoothing term are taken as 0.2 and 5.0 respectively.

257x65 C grid is used for this test case which is the exactly the same as the one used by Tınaztepe[15]. Grid consists of 192 points on the airfoil and 32 points on the wake region. There are 120 grid points on the upper surface and 73 points on

the lower surface of the airfoil. Minimum Δy used in this grid is 0.00001 and Δx is 0.001. Airfoil is clustered around 55% of the where the shock wave is expected to occur. Grid around the airfoil is shown in Figure 5.14.
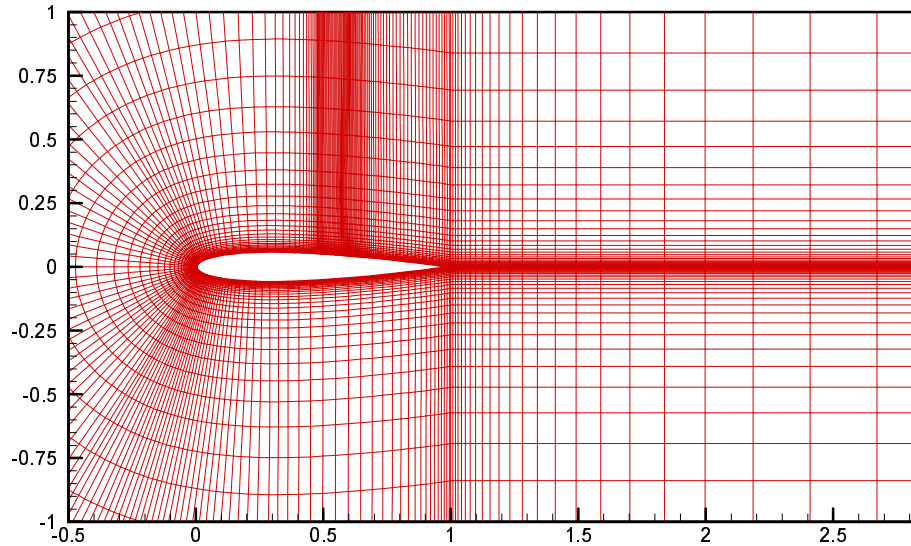

Figure 5.14   C Grid Used For NACA-0012 Transonic Turbulent Flow Test Case

Solutions obtained from both turbulence models are continued until about two orders of decrease is achieved in the x-momentum residual. Solutions are obtained from both turbulence models of Baldwin-Barth and Spalart-Allmaras turbulence models. Both solutions are obtained from uncoupled discretization of turbulence models. The obtained results are compared with the numerical results of Tınaztepe[15]andexperimentalresults.

Results obtained from Baldwin-Barth and Spalart-Allmaras turbulence models are presented in Figures of 5.16, 5.17 and 5.18. It is observed in Mach number plots of both models, there are oscillations around shock wave. Although artificial smoothing terms are used for damping the oscillation around shock waves or discontinuities, after several tests are handled, it is observed that artificial smoothing terms are not enough to prevent oscillations. Moreover, the more increase the second order artificial smoothing term, the worse result gets. Oscillations are also observed in *Cp* plot of the both solutions after the shock wave. There are also

deviations at the lower part of the airfoil on the *Cp* plot of both solutions which is presented in Figure 5.18. In spite of the oscillations and deviations, both models capture the shock wave and capture the shock position better than the Baldwin-Lomax turbulence model solution. In accordance with the Baldwin-Lomax turbulence model solutions obtained by Tınaztepe [15], both models capture the shock position better. In experimental result shock position is about 48% of the chord, in present case both turbulence models predict the shock location at the 53% of the cord and shock location is obtained at about 56% of the cord by Tınaztepe [15]. Conclusively, solver should be enhanced for more complex geometries to acquire more accurate solutions.
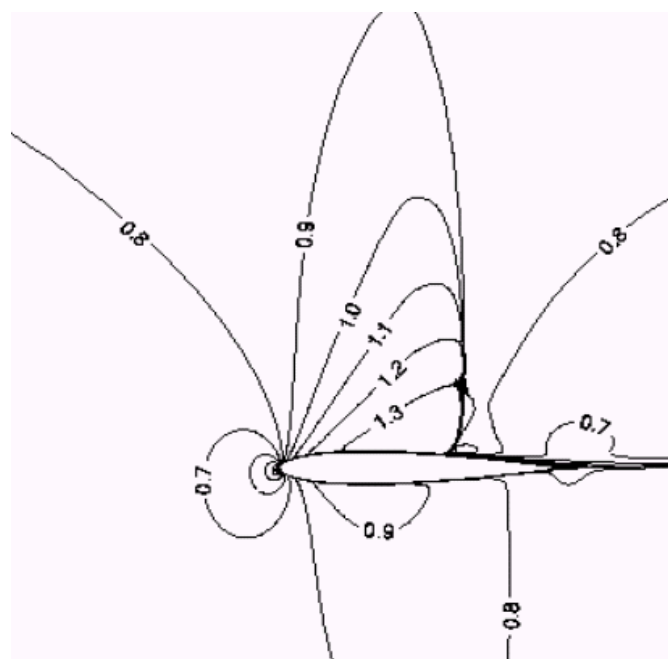

Fig 5.15 Mach Number Contour Plot for the Turbulent Transonic Flow NACA -0012 Test Case (Baldwin-Lomax Solution [15])
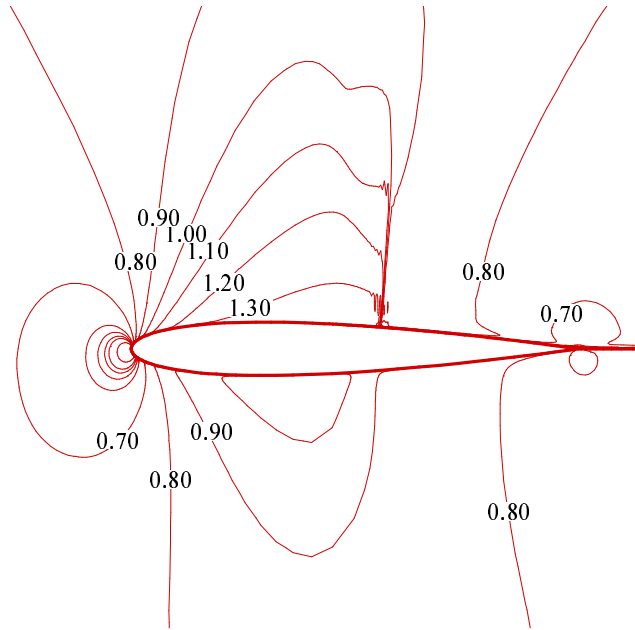
Fig 5.16 Mach Number Contour Plot for the Turbulent Transonic Flow
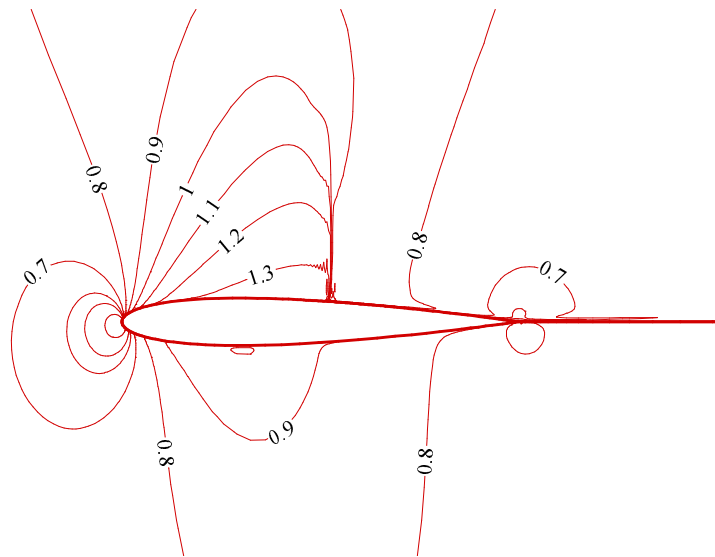NACA -0012 Test Case (Baldwin-Bart Solution)

Fig 5.17 Mach Number Contour Plot for the Turbulent Transonic Flow
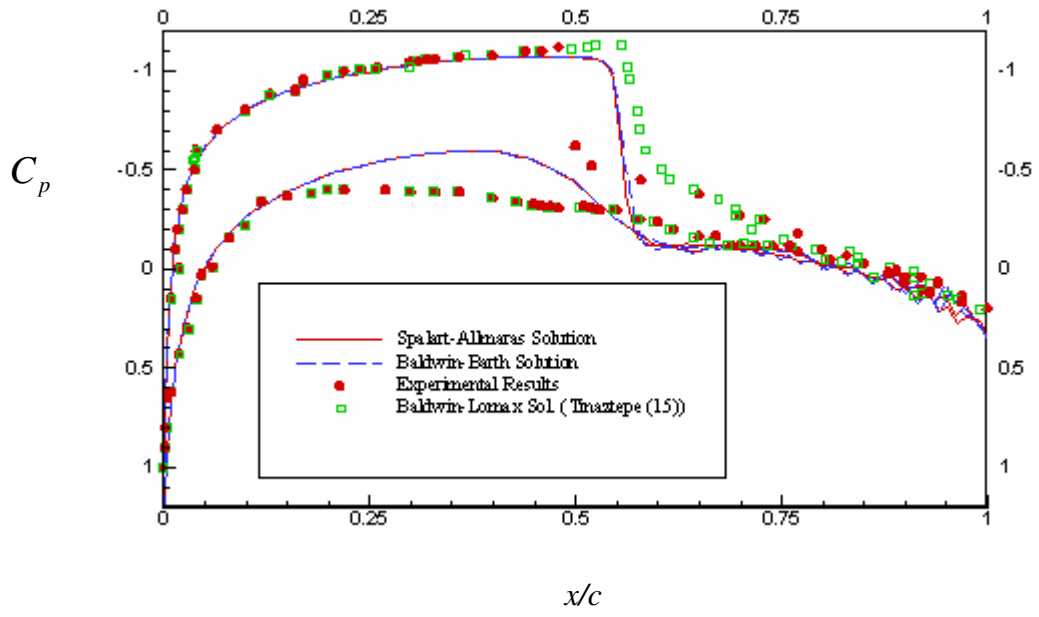NACA -0012 Test Case (Spalart-Allmaras Solution)

Fig 5.18 Calculated Pressure Coefficient Distributions on NACA-0012 Airfoil for the Turbulent Transonic Test Case

CHAPTER 6

DISCUSSION AND CONCLUSION

6.1 SUMMARY AND DISCUSSION

In this study one equation turbulence models namely Baldwin-Bart and Spalart Allmaras eddy viscosity models are implemented into previously developed Navier-Stokes solver.

One equation turbulence models are selected for implementation into Navier-Stokes solver because of their success and popularity. They also do not depend on empirically determined algebraic length scales. Moreover, both zero and two equation turbulence models have some inadequacies. In spite of the fact that two equation models are complete, they have the problems related to numerical implementation [9]. Zero equation models are simple models, they don't consider turbulent history effects and they give poor results in separated flow [9].

In this study three test cases are handled. First test case is the laminar flat plate problem. The main purpose of this test case is to check the validity of the Navier-Stokes solver before implementation of the turbulence models. The obtained results are in good agreement with the analytical solutions and so turbulence models are implemented. The next two test cases handled belong to turbulent flow. Accuracy and performance of the turbulence models are firstly tested over turbulent flat plate problem. The obtained results for the turbulent flat plate test case are satisfactory for both turbulence models. Among the Spalart-Allmaras and Baldwin-Barth turbulence models, best local skin friction coefficient distribution is obtained by Spalart-

Allmaras solution. On the other hand, it observed that obtained results of local skin friction distributions are not better than Baldwin-Lomax turbulence model. Final test case is the transonic flow over NACA-0012 airfoil. This test case is chosen due to the fact that the transonic flow is one of the most challenging test cases in aerodynamics and testing the solver for flow separation case. In transonic test case, although the solver using Baldwin-Barth and Spalart-Allmaras turbulence models captures the shock location more accurate than the Baldwin Lomax turbulence model and show the flow separation, it is observed that there are oscillations on both Mach number and *Cp* plots. For damping these oscillations artificial damping factor is not satisfactory and it is also observed that increasing artificial damping factor effect the solution in bad manner. Moreover, there are deviations at the lower part of the airfoil with respect to the experimental solutions on *Cp* plot. As a conclusion, turbulence models implemented solver has adequate capability of shock capturing and giving solution of turbulent flows but it should be enhanced more for more precise and stable solutions.

6.2. FUTURE RECOMMENDATIONS

First improvement made to this solver will be related to Navier-Stokes solver. Present solver should be enhanced more by addition of a Total Variation Diminishing (TVD) scheme. This will damp oscillation on the graphs and eliminate the necessity of artificial damping terms.

Second and final improvement will be made by increasing speed of convergence. Because of the huge size of grids used for airfoils results obtained are in the order of days. Speed of convergence can be increased by parallel computing techniques and addition of multigrid algorithm.

REFERENCES

[1]   Blazek J., "Computational Fluid Dynamics Principles and Applications", Elsevier, UK, 2001.

[2]   Versteeg, H. K., Malalasekera, W., "An Introduction to Computational Fluid Dynamics, the Finite Volume Method", Longman, 1995

[3]   Bradshaw Peter, "Understanding and prediction of turbulent flow", Int. J. and Fluid Flow, 45-54, 1996

[4]   George W.K., "Lectures in Turbulence for the 21st Century", Lecture notes in Chalmers university of Technology, 2003

[5]   Wilcox, D. C., "Turbulence Modeling for CFD", DCW Industries Inc., USA, 1994.

[6]   Tennekes, H., Lumley J. L., "A First Course in Turbulence", MIT Press, USA, 1994.

[7]   Bradshaw, P. "Turbulence Modelling With Application To Turbomachinery", Prog. Aerospace Science, Vol. 32, pp. 575-624, 1996

[8]   Davidson Lars, "An Introduction to Turbulence Models", Chalmers University of Technology Publication 97/2, November 2003

[9] Baldwin B.S., Barth. T.J., "A One Equation Turbulence Transport Model for High Reynolds Number Wall-Bounded Flows", NASA-TM-102847, August 1990.

[10] El Khoury, M., "An Improved Wall Distance Free Version of the Baldwin-Barth Turbulence Model", Proceedings of IMECE, November 16-21, 2003.

[11] Hoffman, K. A., Chiang, S.T., "Computational Fluid Dynamics", Vol. (1-3) Engineering Education System Publication, USA, August 2000.

[12] Spalart, P.R. and Allmaras, S.R., "One Equation Turbulence Models FOR Aerodynamic Flows", AIAA Paper 92-439, 1992.

[13] Edwards Jack R., Chandra Suresh., "Compression of Eddy Viscoisty-Transport Turbulence Models for Three Dimensional, Shock Seperated Flowfields", AIAA Journal, 1996.

[14] Ni, R.H., "A Multiple-Grid Scheme for Solving the Euler Equations", AIAA Journal, Vol. 20, pp. 1565-71, 1982.

[15] Tınaztepe, H. T., "A Finite Volume Method for Compressible Viscous Flows", Ph. D. Thesis, METU, Turkey, March 1997.

[16] Haliloğlu, M. U, "Development of a Three Dimensional Object Oriented Navier Stokes Solver Using C++ Programming Language", M. Sc. Thesis, METU, Turkey, June 2000.

[17] El Khoury, M., "Development of a Three Dimensional Object Oriented Navier Stokes Solver Using Two Equation Turbulence Models", M. Sc. Thesis, METU, Turkey, June 2001.

[18]   Genç, Balkan Ziya "Implementation and Comparison of Turbulence Models On a Flat Plate Problem Using a Navier Stokes Solver", METU, Turkey, September 2003

[19]   Hirsch C., "Numerical Computation of Internal and External Flows", Vol 1 -2, John Wiley & Sons, Great Britain, 1988-1990.

[20] Mason, W.H., "7.Transonic Aerodynamics of Airfoils and Wings",   Lecture Notes in Virginia Institute of Technology, USA, 2003

APPENDIX

The aim of this section is to define coefficients of Baldwin–Barth turbulence model production term S [19].

$$a_1 = \frac{4}{3}\xi_x{}^2 + \xi_y{}^2 \tag{A1}$$

$$a_2 = \xi_x{}^2 + \frac{4}{3}\xi_y{}^2 \tag{A2}$$

$$a_3 = \frac{1}{3}\xi_x\xi_y \tag{A3}$$

$$a_4 = \xi_x{}^2 + \xi_y{}^2 \tag{A4}$$

$$b_1 = \frac{4}{3}\eta_x{}^2 + \eta_y{}^2 \tag{A5}$$

$$b_2 = \eta_x{}^2 + \frac{4}{3}\eta_y{}^2 \tag{A6}$$

$$b_3 = \frac{1}{3}\eta_x\eta_y \tag{A7}$$

$$b_4 = \eta_x{}^2 + \eta_y{}^2 \tag{A8}$$

$$c_1 = \frac{4}{3}\eta_x\xi_x + \xi_y\eta_y \tag{A9}$$

$$c_2 = \xi_x\eta_x + \frac{4}{3}\xi_y\eta_y \tag{A10}$$

$$c_3 = \eta_x\xi_y - \frac{2}{3}\xi_x\eta_y \tag{A11}$$

$$c_4 = \xi_x \eta_y - \frac{2}{3} \xi_y \eta_x \qquad\qquad\qquad (A12)$$

$$c_5 = \xi_x \eta_x + \xi_y \eta_y \qquad\qquad\qquad (A13)$$